

"Self-inactivating" rabies viruses are susceptible to loss of their intended attenuating modification

Makoto Matsuyama¹, Lei Jin¹, Thomas K. Lavin¹, Heather A. Sullivan¹, YuanYuan Hou¹, Nicholas E. Lea¹, Maxwell T. Pruner¹, María Lucía Dam Ferdínez¹, and Ian R. Wickersham¹

¹McGovern Institute for Brain Research, Massachusetts Institute of Technology, Cambridge, MA

SUMMARY

An article in *Cell* reported a new form of modified rabies virus that was apparently capable of labeling neurons "without adverse effects on neuronal physiology and circuit function" but that nevertheless was able to spread between neurons as efficiently as the widely-used first-generation deletion-mutant (ΔG) rabies viral vectors. The new "self-inactivating" rabies ("SiR") viruses differed from first-generation vectors only by the addition of a destabilization domain to the viral nucleoprotein. We noticed that the transsynaptic tracing results from that article appeared inconsistent with the strategy described in it: specifically, the viruses were able to spread between neurons even in the absence of the exogenous protease that was meant to be required. We hypothesized that the viruses used were actually mutants that had lost the intended addition to the nucleoprotein, making them *de facto* first-generation viruses. We obtained samples of two SiR viruses from the authors and show here that the great majority of viral particles in both the "SiR-CRE" and "SiR-FLPo" samples were mutants that had lost the intended modification, consistent with our hypothesis. We also found that SiR-CRE killed 70% of infected neurons *in vivo* within two weeks, consistent with the prediction that mutants without the intended modification would share the toxic phenotype typical of first-generation rabies viral vectors. We hypothesize that the same or similar mutations were present in the viruses used in the original article and that this explains the paradoxical reported findings. While it may be possible to successfully make SiR viral preparations that are not dominated by such mutants, and while it may also be possible that such intact SiR viruses are indeed nontoxic to neurons, we predict that it will not be possible to replicate the transsynaptic tracing results from the original paper unless using mutants similar to the ones that we report here.

INTRODUCTION

Monosynaptic tracing based on deletion-mutant rabies virus has become an important tool in neuroscience since its introduction in 2007 (1) and remains the only way of labeling neurons directly presynaptic to some targeted group of neurons in the absence of prior hypotheses (2-5). Its core principles are, first, selective infection of the targeted neuronal group with a recombinant rabies virus with a deleted gene (which in all work published to date is the "G" gene encoding its envelope glycoprotein) and, second, *in vivo* complementation of the deletion, by expression of the deleted gene in *trans*, in the targeted starting neurons. With all of its gene products thus present in the starting cells, the virus can fully replicate within them and spreads, as wild-type rabies virus does, to cells directly presynaptic to the initially infected neurons. Assuming that G has not been provided *in trans* in these presynaptic cells too, the deletion mutant (" ΔG ", denoting the deletion of G) virus is unable to spread beyond them, resulting in labeling of just the neurons in the initially targeted population and ones that are directly presynaptic to them (1).

A drawback of these ΔG (or "first-generation" (6)) rabies viruses is that they are cytotoxic (6-8), which has spurred several labs to develop less-toxic versions. Reardon, Murray, and colleagues (8) showed that simply using ΔG rabies virus of a different parent strain — switching from the original SAD B19 strain to the more neuroinvasive CVS N2c strain (9) — decreased

52 toxicity and increased transsynaptic labeling efficiency. Our own group has taken a more drastic
53 approach, recently introducing "second-generation" rabies viruses from which both G and a
54 second gene, "L", encoding the viral polymerase, have been deleted (6). Deletion of L reduces
55 the transcriptional activity of the virus to extremely low levels, eliminating detectable toxicity but
56 necessitating that the viruses encode Cre or FLPo recombinase (instead of more typical payloads
57 such as fluorescent proteins) and are used in reporter mice or in combination with recombinase-
58 dependent adeno-associated viral vectors (AAVs). While we showed in our paper only that these
59 second-generation, " Δ GL" viruses are efficient means of direct retrograde targeting of projection
60 neurons, Δ GL viruses can also be used (as shown in work so far unpublished) for monosynaptic
61 tracing, at the cost of the additional complexity of expressing the second deleted gene in *trans*.

62 In another notable development, Ciabatti et al. reported in a paper published in *Cell* that
63 they had created a nontoxic version of Δ G rabies virus that could be used for monosynaptic tracing
64 with no need to express any additional genes other than G (10). The new virus, termed "self-
65 inactivating rabies" virus or "SiR", was simply a Δ G, SAD B19 strain rabies virus except for one
66 modification: the addition of a destabilization domain to the viral nucleoprotein, encoded by "N",
67 the first gene in the rabies viral genome. This destabilization (or "PEST") domain was linked to
68 the nucleoprotein's C terminus by a short linker containing the cleavage site of tobacco etch virus
69 protease (TEVP). The authors' stated intent was that, in the absence of TEVP, newly-produced
70 nucleoprotein (the indispensable protein which encapsidates the viral genome and without which
71 no transcription or replication can occur) would be rapidly degraded because of the attached
72 destabilization domain and that the transcription and replication activity of the virus would
73 therefore be greatly reduced, making the virus nontoxic. To compensate for this reduction in
74 transcription, the SiR viruses encoded Cre or FLPo recombinases and were used in reporter mice
75 or with reporter AAVs, paralleling our own strategy using Δ GL rabies viruses (6). In the presence
76 of TEVP, however, the destabilization domain would be cleaved from the C terminus of the
77 nucleoprotein, which therefore would not be degraded and would allow normal levels of
78 transcription and replication of the virus. In the words of Ciabatti et al., "the virus should be able
79 to transcribe and replicate only when TEVP is present" (10).

80 While most of the results reported in their paper are consistent with a virus that is
81 conditionally deficient in nucleoprotein production, Ciabatti et al. went on to show that their "SiR"
82 viruses could be used for monosynaptic tracing *in vivo* with no need for TEVP expression at all:
83 the viruses could simply be complemented by G expression in the starting cell population and
84 efficiently spread to putatively presynaptic neurons. In their lack of dependence on TEVP
85 expression, the SiR viruses behaved as if they were simply first-generation, Δ G rabies viruses.
86 This was a paradoxical result: the modified nucleoprotein was supposed to require TEVP-
87 mediated removal of the destabilization domain in order to accumulate in infected cells and allow
88 viral replication, but it appeared not to in the starting cells *in vivo*. Furthermore, despite this
89 apparent ability to replicate perfectly well despite the C-terminal degron that was intended to
90 prevent it from doing so, the virus appeared not to kill neurons: Ciabatti et al. found many surviving
91 putatively-presynaptic neurons at three weeks after rabies virus injection.

92 We hypothesized an alternative explanation for these results, as follows.

93 As an incidental finding from the control experiments in our paper on second-generation
94 (Δ GL) rabies virus (6), we discovered that even first-generation (Δ G) virus could apparently be
95 made significantly less toxic simply by switching the transgene that it encodes from some "normal"
96 one like the tdTomato gene to the coding sequence for Cre recombinase. Following an initial die-
97 off of a fraction of neurons infected with a Cre-encoding Δ G virus, a comparably large fraction
98 survived for four months, the longest we followed them, with modest physiological changes in
99 some (6). These findings suggested a "quick and dirty" way of making a less-toxic, but by no
100 means completely nontoxic, monosynaptic tracing system: use a first-generation, Δ G rabies virus
101 encoding a recombinase and do the experiments in reporter mice.

102 We hypothesized that Ciabatti et al. had inadvertently done exactly that. Rhabdoviruses
103 have high mutation rates (11-16), and production of high-titer rabies virus stocks for *in vivo*
104 injection typically involves repeated passaging on complementing cell lines (17-19), which affords
105 ample opportunity for accumulation of mutants with a selective replication advantage. We
106 therefore hypothesized that the viruses that Ciabatti et al. had actually ended up with and used
107 for their transsynaptic tracing experiments were mutants with premature stop codons at or near
108 the end of the native nucleoprotein gene and before the sequence of the destabilization domain.

109 If Ciabatti et al.'s viruses had lost the intended C-terminal addition because of mutation,
110 their "SiR-CRE" virus would in practice be a simple first-generation, ΔG rabies viral vector
111 expressing Cre. Because we have shown that such a virus can leave a large percentage of
112 infected cells alive, the presence of surviving cells even at long time points would have led the
113 authors to conclude that they had developed a new kind of rabies virus that did not kill cells but
114 that could be used for monosynaptic tracing by simple complementation by G alone.

115 Here we show that, in both of the two SiR virus samples to which we had access, the vast
116 majority of viral particles did have mutations in their genomes that caused the complete loss of
117 the intended C-terminal addition to the nucleoprotein, so that they were effectively just ordinary
118 first-generation ΔG rabies viral vectors. We also tested the SiR-CRE virus *in vivo* and found that
119 it was rapidly cytotoxic.

120

121 RESULTS

122

123 We analyzed samples of two viruses sent directly from the Tripodi lab to MIT in September
124 2017, two months after the publication in which they were introduced (10): "EnvA/SiR-CRE"
125 (made from genome plasmid Addgene 99608, pSAD-F3-NPEST-iCRE-2A-mCherryPEST) and
126 "EnvA/SiR-FLPo" (made from genome plasmid Addgene 99609, pSAD-F3-NPEST-FLPo-2A-
127 mCherryPEST). These two viruses, like all of the other rabies viruses described in Ciabatti et al.,
128 have the SAD B19 strain of rabies virus as their parent strain. Both of the viruses sent by the
129 Tripodi lab had been packaged with the avian and sarcoma virus subgroup A envelope
130 glycoprotein ("EnvA") for targeted infection of cells expressing EnvA's receptor, TVA (1).

131 For comparison with the two SiR viruses, we made five control viruses in our own
132 laboratory: three first-generation vectors RV ΔG -4Cre (6), RV ΔG -4FLPo (see Methods), and
133 RV ΔG -4mCherry (20), and two second-generation vectors RV ΔGL -4Cre and RV ΔGL -4FLPo (6).
134 All of these viruses are also on the SAD B19 background, like the SiR viruses. For each of the
135 four recombinase-expressing viruses from our laboratory, we made one preparation packaged
136 with the EnvA envelope protein and one preparation packaged with the native rabies virus (SAD
137 B19 strain) glycoprotein (denoted as "B19G"); RV ΔG -4mCherry (used only as a control for the
138 Sanger sequencing) was packaged just with the EnvA envelope protein.

139

140 Sequencing of viral genomes: Sanger sequencing

141

142 In order to directly test our hypothesis that the SiR viruses had developed premature stop
143 codons removing the PEST domain in a majority of viral particles, we sequenced the genomes of
144 a large number of individual viral particles using two different techniques.

145 First, we used ordinary Sanger sequencing to determine the sequence in the vicinity of
146 the end of the nucleoprotein gene for 50 – 51 individual viral particles of each of the two SiR
147 viruses and for a first-generation virus from our own laboratory, RV ΔG -4mCherry (Figure 1). We
148 ensured the isolation of individual viral genomes by using a primer with a random 8-base index
149 for the reverse transcription step, so that the cDNA copy of each RNA viral genome would have
150 a unique index. Following the reverse transcription step, we amplified the genomes by standard
151 PCR, cloned the amplicons into a generic plasmid, transformed this library into *E. coli* and

152 sequenced plasmids purified from individual colonies. As shown in Figure 1, the results confirmed
153 our hypothesis that SiR viruses are prone to loss of the C-terminal addition to the nucleoprotein.

154 Specifically, in the SiR-CRE sample, 100% of the 51 sequenced viral particles had lost the
155 PEST domain. Fifty out of the 51 had the same point mutation in the linker between the end of
156 the native nucleoprotein gene and the TEVP cleavage site, converting a glycine codon (GGA) to
157 a stop codon (TGA) so that the only modification to the C-terminus of the nucleoprotein was the
158 addition of two amino acids (a glycine and a serine). The one sequenced viral particle that did not
159 have this point mutation had a single-base insertion in the second-to-last codon of the native
160 nucleoprotein gene, frameshifting the rest of the sequence and resulting in 15 amino acids of
161 nonsense followed by a stop codon before the start of the PEST domain sequence.

162 In the SiR-FLPo sample, the population was more heterogeneous: out of 50 sequenced
163 viral particles, 18 had the same stop codon that was found in almost all genomes in the Cre
164 sample, while another 28 had a different stop codon three amino acids upstream, immediately at
165 the end of the native nucleoprotein gene (converting a serine codon (TCA) to a stop codon (TGA)).
166 Four viral particles had no mutations in the sequenced region. Thus 46/50 (92%) of the SiR-FLPo
167 viral particles sequenced had lost the PEST domain.

168 In contrast, in the first-generation virus from our own lab, RV Δ G-4mCherry, none of the 50
169 viral particles sequenced had mutations in the sequenced region on the end of the nucleoprotein
170 gene.

171

172 **Sequencing of viral genomes: Single-molecule, real-time (SMRT) sequencing**

173

174 As a second approach to analyzing the mutations present in the SiR viruses, we employed
175 a large-scale sequencing technology: single-molecule, real-time ("SMRT") sequencing, which
176 provides independent sequences of tens of thousands of individual single molecules in a sample
177 in parallel (Figure 2). The results from this advanced sequencing method were quite consistent
178 with the results from the Sanger sequencing presented above. As with the sample preparation for
179 Sanger sequencing, we included a random index (10 bases, in this case) in the reverse
180 transcription primer, so that again the cDNA copy of each RNA viral genome molecule would be
181 labeled with a unique index.

182 SMRT sequencing entails circularization of the DNA amplicons and multiple consecutive
183 passes around the resulting circular molecule, with the redundancy provided by this repeated
184 sequencing of each position increasing the signal to noise ratio and statistical significance of the
185 results. The numbers presented in Figure 2 and below use the default of including only clones
186 that had at least three reads of each base ("circular consensus sequence 3", or "CCS3" in
187 Supplementary File S3). Using the increasingly stringent criteria of requiring either five or eight
188 reads per base (CCS5 or CCS8) reduced the numbers of qualifying genomes in all cases and
189 changed the percentages slightly but gave very similar results overall. Because read accuracy for
190 SMRT sequencing is $\geq 98\%$ for circular consensus sequencing with 3 passes (see
191 [https://www.mscience.com.au/upload/pages/pacbio/technical-note---experimental-design-for-](https://www.mscience.com.au/upload/pages/pacbio/technical-note---experimental-design-for-targeted-sequencing.pdf)
192 [targeted-sequencing.pdf](https://www.mscience.com.au/upload/pages/pacbio/technical-note---experimental-design-for-targeted-sequencing.pdf)), we used a conservative threshold of 2% frequency of any given point
193 mutation position in order to screen out false positives. Also to be very conservative, for Figure 2
194 we ignored all apparent frame shifts caused by insertions and deletions, because insertions in
195 particular are prone to false positives with SMRT sequencing (21). See Supplementary File S3
196 for details, including details of frameshifts due to insertions; Supplementary Files S4-S6 contain
197 the sequences of the PCR amplicons that would be expected based on published sequences of
198 the three viruses, but to summarize here:

199 As a control, we used a virus from our own laboratory, RV Δ G-4Cre (6) (see Addgene
200 #98034 for reference sequence). Out of 17,978 sequenced genomes of this virus, we found no
201 mutations above threshold frequency at the end of N. We did find that 1,706 viral particles (9.49%)
202 had a nonsynonymous mutation (TCT (Ser) \rightarrow ACT (Thr)) farther up in N at amino acid position

203 419 (31 amino acids upstream of the end of the 450-aa native protein). We do not know if this
204 mutation is functionally significant, although it is not present in CVS N2c (22), HEP-Flury (23),
205 ERA (24), or Pasteur strains (Genbank GU992320), so these particles may effectively be N-
206 knockouts that were propagated by coinfection with virions with intact N (see Discussion for more
207 on such parasitic co-propagating mutants).

208 For the SiR-CRE virus, out of 22,205 viral genomes sequenced, 22,032 had the premature
209 stop codon (GGA -> TGA) in the linker between the native nucleoprotein gene and the TEVP
210 cleavage site sequence. In other words, even without including frameshifts, at least 99.22% of
211 the individual viral particles in the SiR-CRE sample were simply first-generation ΔG vectors.

212 For the SiR-FLPo virus, out of 17,086 viral genomes sequenced, 5,979 had the stop codon
213 (GGA -> TGA) in the linker, 8,624 had the stop codon (TCA -> TGA) at the end of N, and a further
214 28 had a different stop codon (TCA -> TAA) at the same position at the end of N. Of these, 305
215 viral particles had premature stop codons at both of these two positions, so that the total number
216 of viral particles with one or both stop codons immediately before the PEST domain was $(8624 +$
217 $5979 + 28 - 305 = 14,326)$. In other words, at least 83.85% of the individual viral particles in the
218 SiR-FLPo sample were simply first-generation ΔG vectors, with the only modification of the
219 nucleoprotein being either two amino acids added to, or one amino acid lost from, the C-terminus.

220

221 **Anti-nucleoprotein immunostaining**

222

223 We infected reporter cell lines with serial dilutions of the two EnvA-enveloped SiR viruses
224 as well as the eight recombinase-expressing ones from our own lab: ΔG vs. ΔGL , Cre vs. FLPo,
225 EnvA vs. B19G envelopes. Three days later, we immunostained the cells for rabies virus
226 nucleoprotein and imaged the cells with confocal microscopy.

227 As seen in Figure 3, we found that the cells infected with the SiR viruses looked very
228 similar to those infected with the first-generation, ΔG viruses. Notably, the viral nucleoprotein,
229 which in the SiR viruses is intended to be destabilized and degrade rapidly in the absence of
230 TEVP, accumulated in the SiR-infected cells in clumpy distributions that looked very similar to
231 those in the cells infected with the first-generation, ΔG viruses. By contrast, the cells infected with
232 the second-generation, ΔGL viruses, which we have shown to be noncytotoxic (6), did not show
233 any such nucleoprotein accumulation, clumped or otherwise, only punctate labeling presumably
234 indicating isolated viral particles or post-infection uncoated viral particles (ribonucleoprotein
235 complexes) that are not replicating.

236

237 **Longitudinal two-photon imaging *in vivo***

238

239 To see whether the SiR viruses kill neurons in the brain, we conducted longitudinal two-
240 photon imaging *in vivo* of virus-labeled neurons in visual cortex of tdTomato reporter mice, as we
241 had done previously to demonstrate the nontoxicity of second-generation rabies virus (6) (Figure
242 4). Because the SiR viruses were EnvA-enveloped, we first injected a lentivirus expressing EnvA's
243 receptor TVA, then one week later we injected either SiR-CRE or one of two EnvA-enveloped
244 viruses made in our laboratory: the first-generation virus RV ΔG -4Cre(EnvA) or the second-
245 generation virus RV ΔGL -4Cre(EnvA). Beginning one week after rabies virus injection, we imaged
246 labeled neurons at the injection site every seven days for four weeks, so that we could track the
247 fate of individual neurons over time.

248 As we found in our previous work (6), our second-generation virus RV ΔGL -4Cre did not
249 kill neurons to any appreciable degree: all but a tiny handful of the neurons labeled by this virus
250 at seven days after injection were still present three weeks later in all mice. Again as we have
251 found previously (6), our first-generation virus RV ΔG -4Cre did kill neurons, but by no means all
252 of them (see the Discussion for a possible reason for this).

253 However, we found that the putatively nontoxic SiR-CRE caused a steep loss of neurons
254 much more pronounced than even our first-generation virus did. By 14 days after injection, 70%
255 of cells seen at seven days were dead; by 28 days, 81% were.

256 There is a possible confound from our use of the tdTomato reporter line Ai14 (which we
257 used primarily because we already had large numbers of mice of this line): because SiR-CRE is
258 actually "SiR-iCRE-2A-mCherryPEST", designed to coexpress mCherry (with an added C-
259 terminal PEST domain intended to destabilize it, as for the nucleoprotein) along with Cre, it is
260 conceivable that some of the SiR-CRE-labeled red cells at seven days were only expressing
261 mCherry and not tdTomato. If the destabilized mCherry were expressed only transiently, as
262 Ciabatti et al. intended it to be (10), and a significant fraction of SiR-CRE virions had mutations in
263 the Cre gene so they did not express functioning Cre, then it is possible that some of the red cells
264 seen at seven days were labeled only with mCherry that stopped being visible by 14 days, so that
265 it would only look like those cells had died.

266 We viewed this alternative explanation as unlikely, because Ciabatti et al. injected SiR-
267 CRE in an EYFP reporter line and found no cells labeled only with mCherry and not EYFP at six
268 days and nine days postinjection (see Figure S4 in Ciabatti et al.). Nevertheless, we addressed
269 this potential objection in several ways.

270 First, we sequenced the transgene inserts (iCre-P2A-mCherryPEST) of 21 individual SiR-
271 CRE viral particles (see Supplementary File S1) and found that only two out of 21 had mutations
272 in the Cre gene, suggesting that there would not have been a large population of cells only labeled
273 by mCherry and not by tdTomato.

274 Second, we repeated some of the SiR-CRE injections and imaging in a different reporter
275 line: Ai35, expressing Arch-EGFP-ER2 after Cre recombination (25) (Jax 012735). Although we
276 found that the membrane-localized green fluorescence from the Arch-EGFP-ER2 fusion protein
277 was too dim and diffuse at seven days postinjection to be imaged clearly, we were able to obtain
278 clear images of a number of cells at 11 days postinjection. We found that 46% of them had
279 disappeared only three days later (see Figure 5 and Supplementary Video S1), and 86% had
280 disappeared by 28 days postinjection, consistent with a rapid die-off. Furthermore, we found that
281 the red fluorescence in Ai35 mice, which was due only to the mCherry expressed by the virus,
282 was much dimmer than the red fluorescence in Ai14 mice at the same time point of seven days
283 postinjection and with the same imaging parameters (see Supplementary Figure S1): the mean
284 intensity was 45.86 (arbitrary units, or "a.u.") in Ai14 but only 16.29 a.u. in Ai35. This is consistent
285 with the published findings that tdTomato is a much brighter fluorophore than mCherry (26),
286 particularly with two-photon excitation (27), and it is also consistent with Ciabatti et al.'s addition
287 of a destabilization domain to mCherry's C-terminus (although we also observed that there were
288 still red fluorescent cells present at week four in Ai35 (data not shown)). We therefore redid the
289 counts of labeled cells in our Ai14 datasets to include only cells with fluorescence at seven days
290 of more than 32.33 a.u., the midpoint of the mean intensities in Ai35 versus Ai14 mice, in order to
291 exclude neurons that might have been labeled with mCherry alone. As seen in Figure S2,
292 restricting the analysis to the cells that were brightest at seven days (and therefore almost
293 certainly not labeled with just mCherry instead of either just tdTomato or a combination of both
294 mCherry and tdTomato) made no major difference: 70.0% of SiR-labeled neurons had
295 disappeared by 14 days, and 80.8% were gone by 21 days.

296 Although in theory it is possible that the disappearance of the infected cells could be due
297 to cessation of tdTomato or Arch-EGFP-ER2 expression rather than to the cells' deaths, because
298 of downregulation by rabies virus of host cell gene expression (28), we view this as highly unlikely.
299 Downregulation of host cell gene expression by rabies virus is neither total ("cells with high
300 expression of RbV transcripts retain sufficient transcriptional information for their classification
301 into a specific cell type." (28)) nor uniform (29); in practice, we saw no evidence of a decline in
302 reporter expression in the infected cells but in fact found the exact opposite. As can be seen in a
303 number of cells in Figures 2 and S3, the cells got brighter and brighter over time, unless they

304 abruptly disappeared. In our experience, including in this case, cells infected with rabies virus
305 increase in brightness until they die, often blebbing and coming apart into brightly labeled pieces,
306 regardless of whether the fluorophore is expressed from a reporter allele (as in this case) or
307 directly by the virus (see Chatterjee et al. 2018 for many more examples of this (6)).

308
309

310 DISCUSSION

311

312 Although many of the results presented in Ciabatti et al. (10) seemed internally consistent, the
313 results showing transsynaptic tracing were puzzling. The degron fused to the C terminus of the
314 nucleoprotein was supposed to require removal by TEV protease in order to allow replication of
315 the SiR virus, but the authors reported that the viruses spread efficiently *in vivo* with no TEV
316 protease present at all. The results that we have shown here suggest that the likely explanation
317 is that the SiR viruses had simply lost the intended C-terminal modification of the nucleoprotein
318 through mutation, as we found had happened in both of the two viruses given to us by the authors
319 shortly after publication of their paper.

320 While it is possible that the escape of the two SiR virus samples from the modification
321 intended to attenuate them was a fluke due to bad luck with those two batches, we view this as
322 unlikely, for the following three reasons. First, both of the two SiR virus samples to which we had
323 access had independently developed mutations causing loss of the intended C-terminal addition
324 to the nucleoprotein: we know that the mutations were independent because the two samples
325 were of different viruses so did not both derive from a single compromised parental stock. Second,
326 the mutation profiles of the two viruses were very different: whereas the SiR-CRE sample had the
327 same point mutation in nearly 100% of its viral particles, only a minority of the SiR-FLPo particles
328 had that particular mutation, with the majority having a different point mutation three codons away
329 that had the same result. This suggests that any of the many opportunities for removing the C-
330 terminal addition — creation of a premature stop codon at any one of a number of sites, or a
331 frameshift mutation anywhere in the vicinity — can be exploited by a given batch of virus, greatly
332 increasing the probability of such mutants arising. Third, Ciabatti et al.'s finding that viral
333 replication and spread occurred *in vivo* in the absence of TEVP is difficult to understand in the
334 absence of mutations but is easily explained if the viral preparations used for those experiments
335 harbored the kind of mutations that we found in the two preparations to which we had access.

336 If the viruses used for the otherwise-unexplained transsynaptic tracing experiments in
337 Ciabatti et al. were actually *de facto* first-generation ΔG viruses like the SiR samples that we
338 analyzed, how could the authors have found, in postmortem tissue, cells labeled by SiR-CRE that
339 had survived for weeks? The answer may simply be that, as we have shown in Chatterjee et al.
340 (6) and again here (Figure 4), a preparation of first-generation rabies viral vector expressing Cre
341 can leave a large fraction of labeled cells alive for at least months, in stark contrast to similar ones
342 encoding tdTomato (6) or EGFP (7). Similarly, Gomme et al. found long-term survival of some
343 neurons following infection by a replication-competent rabies virus expressing Cre (30)).

344 The reason, in turn, why a preparation of a simple ΔG rabies virus encoding Cre can leave
345 many cells alive may be that not all the virions are in fact first-generation viral particles, due,
346 fittingly, to the same high mutation rate that we have highlighted in this paper. We have shown in
347 Chatterjee et al. (6) that a second-generation (ΔGL) rabies virus, which has both its glycoprotein
348 gene G and its polymerase gene L deleted, leaves cells alive for the entire four months that we
349 followed them. However, any first-generation (ΔG) virus that contains a frameshift or point
350 mutation knocking out L will in practice be a ΔGL virus. Indeed, a stop codon or frameshift
351 mutation in the several other viral genes is likely to have a similar effect as one in L (and it might
352 be that the Ser419Thr mutation that we found in 9.49% of our RV ΔG -4Cre virions is just such a
353 knockout mutation of N). Together with the high mutation rate of rabies virus, this means that,
354 within every preparation of first-generation rabies virus there is almost guaranteed to be a

355 population of *de facto* second-generation variants mixed in with the intended first-generation
356 population and propagated in the producer cells by complementation by the first-generation
357 virions. Any rabies virus preparation (whether made in the laboratory or occurring naturally) can
358 be expected to contain a population of such knockout (whether by substitution, frameshift, or
359 deletion) mutants (related to the classic phenomenon of "defective interfering particles", or
360 mutants with a marked replication advantage (31-33), and the higher the multiplicity of infection
361 when passaging the virus, the higher the proportion of such freeloading viral particles typically will
362 be. This would not necessarily be noticed in the case of a virus encoding a more common
363 transgene product such as a fluorophore, because the expression levels of these by the knockout
364 mutants would be too low to label cells clearly (see Figure 1 in Chatterjee et al. (6)). However,
365 with Cre as the transgene, any "second-generation" particles would be able to label neurons but
366 not kill them, because second-generation rabies viral vectors do not kill cells for at least months
367 (6). This explanation would predict that the percentage of neurons surviving infection with a rabies
368 virus encoding Cre will depend on the particular viral preparation that is injected, with some having
369 a greater fraction of knockout particles than others.

370 This could explain why the SiR-CRE virus sample killed cells faster than our own RV Δ G-
371 4Cre (Figure 4). This analysis would also presumably apply to first-generation (Δ G) viruses
372 expressing FLPo: while we found that the FLPo-expressing version that we made did not leave
373 as many cells alive as the Cre-expressing version (Supplementary Figure S3) did, that preparation
374 may simply have had fewer mutants with knockout of genes essential for replication. It is unclear
375 whether Ciabatti et al.'s SiR-FLP would leave many cells alive for long durations, as the authors
376 did not show any results indicating that it does, and we did not test it *in vivo* ourselves.

377 To summarize, we have found that both of the SiR virus samples that we analyzed
378 consisted overwhelmingly of mutants that had lost the modification that was intended to make
379 them nontoxic. We believe that this provides the most likely explanation for Ciabatti et al.'s
380 paradoxical results. However, because we don't know for certain that the viruses that Ciabatti et
381 al. used for their paper had the same problem as did the stocks that they gave us, we cannot rule
382 out the following three-part alternative explanation: first, that their transsynaptic tracing
383 experiments were in fact performed with unmutated viruses that only expressed nucleoprotein
384 molecules with intact PEST domains fused to their C termini; second, that these PEST domains,
385 contrary to their intended behavior, did not cause rapid degradation of the nucleoprotein but
386 instead allowed it to accumulate sufficiently to result in viral replication and spread; third, that the
387 large (159 aa) C-terminal addition did not noticeably interfere with the function of the
388 nucleoprotein, with the result that the modified viruses spread just as efficiently as the unmodified
389 versions, even in the absence of TEVP.

390 We regard this alternative explanation as implausible, for the reasons discussed above.
391 However, because of this uncertainty, the conservative conclusions from our findings are simply
392 that SiR viruses are susceptible to loss of their intended modification and that the approach should
393 be used with caution and that the published results should be reinterpreted in light of our findings.
394 We further submit that, because there is currently no evidence that the viruses from the original
395 paper were not mutants like both of the batches that we analyzed, the ability of an intact SiR virus
396 to spread transsynaptically, with or without TEVP, remains unproven.

397 To be clear, we have no reason to believe that it is impossible to make a rabies virus with
398 the C-terminal addition to the nucleoprotein that Ciabatti et al. had intended. A number of groups
399 have made recombinant rabies viruses — as well as other rhabdoviruses and other
400 nonsegmented negative-strand RNA viruses — encoding fusions of exogenous proteins to viral
401 proteins (34-44). However, most of these groups have found that the additions significantly
402 impaired the function of the viral proteins. Most relevantly, an attempt to make SAD B19 rabies
403 virus with EGFP fused to the C terminus of the nucleoprotein was unsuccessful, suggesting that
404 the nucleoprotein is intolerant of large C-terminal additions; the authors of that paper resorted

405 instead to making virus encoding the fusion protein *in addition to the wild-type nucleoprotein*
406 because the fusion protein was evidently dysfunctional (37).

407 These prior attempts have also found that rhabdoviruses can rapidly lose C-terminal
408 portions of viral or exogenous proteins. A vesicular stomatitis virus with GFP fused to the C
409 terminus of the glycoprotein gene lost the modification within a single passage of the virus
410 because of a point mutation creating a premature stop codon (34). Relatedly, a VSV with its
411 glycoprotein gene replaced with that of a different virus was found to quickly develop a premature
412 stop codon causing loss of the last 21 amino acids of the exogenous glycoprotein, conferring a
413 marked replication advantage to the mutants bearing the truncated version (45).

414 Generalizing from these prior examples as well as our findings here, we suggest that any
415 attempt to attenuate a virus by addition to the C terminus of a viral protein will be vulnerable to
416 loss of the addition by creation of either a stop codon or a frameshift, and that any such virus will
417 therefore need to be monitored very carefully.

418 Despite this, we do not claim that it is impossible, given sufficient care, to make SiR virus
419 with the intended C-terminal addition intact in the great majority of viral particles. A good way to
420 start might be to make synonymous mutations to the codons that had most frequently mutated in
421 the stocks that we analyzed, so that those codons are not a single point mutation away from a
422 stop codon (e.g., GGA -> GGG, TCA -> TCT); this improvement would not prevent loss of the C-
423 terminal addition due to frameshift mutations, however.

424 Indeed, in response to our posting a preprint of an earlier version of this manuscript in
425 February 2019 (46), the authors of the original paper have recently posted a new preprint in which
426 they report that they are now able to make mutation-free SiR virus and that this intact SiR virus is
427 noncytotoxic when used to directly infect cortical neurons (47). This is a good start but does not
428 change anything about our findings, conclusions, and predictions. Crucially, the new preprint does
429 not include any results testing whether the intact SiR virus can spread transsynaptically, either
430 with TEVP or without it. This suggests that, in over 1.5 years since we brought the problem to
431 light, Ciabatti et al. have not replicated, with unmutated virus, the experiments from their original
432 paper.

433 We predict that they will not be able to. Specifically: it may be the case that an intact SiR
434 virus is capable of at least some transsynaptic spread if provided with both G and TEVP, although
435 again there are no experiments presented either in Ciabatti et al.'s original paper or in their new
436 preprint that tested this, so whether this phenomenon occurs at all, and with what efficiency if it
437 does occur, are currently unknown. We predict, though, that any such intact SiR virus will be
438 incapable of appreciable transsynaptic spread in the *absence* of TEVP, i.e., under the conditions
439 Ciabatti et al. described in *Cell*. To put it another way, we predict that any SiR virus that is found
440 to be capable of efficient transsynaptic spread under the conditions described in Ciabatti et al. '17
441 — i.e., without provision of TEVP — will, if closely examined, be found to consist largely of "escape
442 mutants" similar to those that we have described here.

443

444

445 **METHODS**

446

447 **Cloning**

448 Lentiviral transfer plasmids were made by cloning, into pCSC-SP-PW-GFP (48) (Addgene
449 #12337), the following components:

450

451 the CAG promoter (49) and a Cre-dependent "FLEX" (50) construct consisting of pairs of
452 orthogonal lox sites flanking a back-to-back fusion of the gene for mTagBFP2 (51) immediately
453 followed by the reverse-complemented gene for mCherry (26), to make the Cre reporter construct
454 pLV-CAG-FLEX-BFP-(mCherry)';

455

456 the CAG promoter (49) and a Flp-dependent "FLEX" (50) construct consisting of pairs of
457 orthogonal FRT sites (52) flanking a back-to-back fusion of the gene for mTagBFP2 (51)
458 immediately followed by the reverse-complemented gene for mCherry (26), to make the Flp
459 reporter construct pLV-CAG-F14F15S-BFP-(mCherry)';

460
461 the ubiquitin C promoter from pUB-GFP (53) (Addgene 11155) and the long isoform of TVA (54)
462 to make the TVA expression vector pLV-U-TVA950.

463
464 The first-generation vector genome plasmid pRV Δ G-4FLPo was made by cloning the FLPo gene
465 (55) into pRV Δ G-4Cre.

466
467 The above novel plasmids have been deposited with Addgene with accession numbers 115234,
468 115235, 115236, and 122050.

469
470 **Production of lentiviral vectors**

471 Lentiviral vectors were made by transfection of HEK-293T/17 cells (ATCC 11268)
472 as described (56) but with the use of the vesicular stomatitis virus envelope expression plasmid
473 pMD2.G (Addgene 12259) for all vectors except for LV-U-TVA950(B19G), which was made using
474 the rabies virus envelope expression plasmid pCAG-B19GVSVGCD (56). Lentiviral vectors
475 expressing fluorophores were titered as described (57); titers of LV-U-TVA950(VSVG) and LV-U-
476 TVA950(B19G) were assumed to be approximately the same as those of the fluorophore-
477 expressing lentiviral vectors produced in parallel.

478
479 **Production of titering cell lines**

480 To make reporter cell lines, HEK-293T/17 cells were infected with either pLV-CAG-FLEX-BFP-
481 (mCherry)' or pLV-CAG-F14F15S-BFP-(mCherry)' at a multiplicity of infection of 100 in one 24-
482 well plate well each. Cells were expanded to 2x 15cm plates each, then sorted on a FACS Aria
483 to retain the top 10% most brightly blue fluorescent cells. After sorting, cells were expanded again
484 to produce the cell lines 293T-FLEX-BC and 293T-F14F15S-BC, reporter lines for Cre and FLPo
485 activity, respectively. TVA-expressing versions of these two cell lines were made by infecting one
486 24-well plate well each with LV-U-TVA950(VSVG) at an MOI of approximately 100; these cells
487 were expanded to produce the cell lines 293T-TVA-FLEX-BC and 293T-TVA-F14F15S-BC.

488
489 **Production and titering of rabies viruses**

490 RV Δ G-4Cre and RV Δ GL-4Cre were produced as described (6, 19), with EnvA-enveloped viruses
491 made by using cells expressing EnvA instead of G for the last passage. Titering and infection of
492 cell lines with serial dilutions of viruses was as described (17), with the 293T-TVA-FLEX-BC and
493 293T-TVA-F14F15S-BC lines used for B19G-enveloped viruses and the 293T-TVA-FLEX-BC and
494 293T-TVA-F14F15S-BC used for the EnvA-enveloped viruses. For the *in vivo* injections, the three
495 EnvA-enveloped, Cre-encoding viruses were titered side by side, and the two higher-titer viruses
496 were diluted so that the final titer of the injected stocks of all three viruses were approximately
497 equal at 1.39E9 infectious units per milliliter.

498
499 **Immunostaining**

500 Reporter cells (see above) plated on coverslips coated in poly-L-lysine (Sigma) were infected with
501 serial dilutions of RV Δ G-4Cre and RV Δ GL-4Cre as described (17). Three days after infection,
502 cells were fixed with 2% paraformaldehyde, washed repeatedly with blocking/permeabilization
503 buffer (0.1% Triton-X (Sigma) and 1% bovine serum albumin (Sigma) in PBS), then labeled with
504 a blend of three FITC-conjugated anti-nucleoprotein monoclonal antibodies (Light Diagnostics
505 Rabies DFA Reagent, EMD Millipore 5100) diluted 1:100 in blocking buffer for 30 minutes,
506 followed by further washes in blocking buffer, then finally briefly rinsed with distilled water and air-

507 dried before mounting the coverslips onto microscope slides with Prolong Diamond Antifade
508 (Thermo P36970) mounting medium. Images of wells at comparable multiplicities of infection
509 (~0.1) were collected on a Zeiss 710 confocal microscope.

510

511 **Virus injections and surgery**

512 All experimental procedures using mice were conducted according to NIH guidelines and were
513 approved by the MIT Committee for Animal Care (CAC). Mice were housed 1-4 per cage under a
514 normal light/dark cycle for all experiments.

515

516 Adult (>9 weeks, male and female) Cre-dependent tdTomato reporter Ai14 (58) (Jackson
517 Laboratory #007908) or Arch-EGFP reporter Ai35D (25) (Jackson Laboratory # 012735) mice
518 were anesthetized with isoflurane (4% in oxygen) and ketamine/xylazine (100mg/kg and 10mg/kg
519 respectively, i.p.). Mice were given preemptive analgesics buprenorphine (0.1 mg/kg s.q.) and
520 meloxicam (2 mg/kg s.q.) as well as eye ointment (Puralube); the scalp was then shaved and
521 mice mounted on a stereotaxic instrument (Stoelting Co.) with a hand warmer (Heat Factory)
522 underneath the animal to maintain body temperature. Following disinfection with povidone-iodine,
523 an incision was made in the scalp, and a 3 mm craniotomy was opened over primary visual cortex
524 (V1). 300 nl of LV-U-TVA950(B19G) (see above) was injected into V1 (-2.70 mm AP, 2.50 mm
525 LM, -0.26 mm DV; AP and LM stereotaxic coordinates are with respect to bregma; DV coordinate
526 is with respect to brain surface) using a custom injection apparatus comprised of a hydraulic
527 manipulator (MO-10, Narishige) with headstage coupled via custom adaptors to a wire plunger
528 advanced through pulled glass capillaries (Wiretrol II, Drummond) back-filled with mineral oil and
529 front-filled with virus solution. Glass windows composed of a 3mm-diameter glass coverslip
530 (Warner Instruments CS-3R) glued (Optical Adhesive 61, Norland Products) to a 5mm-diameter
531 glass coverslip (Warner Instruments CS-5R) were then affixed over the craniotomy with Metabond
532 (Parkell). Seven days after injection of the lentiviral vector, the coverslips were removed and 300
533 nl of one of the three EnvA-enveloped rabies viral vectors (with equalized titers as described
534 above) was injected at the same stereotaxic coordinates. Coverslips were reapplied and custom
535 stainless steel headplates (eMachineShop) were affixed to the skulls around the windows.

536

537 ***In vivo* two-photon imaging and image analysis**

538 Beginning seven days after injection of each rabies virus and continuing every seven days up to
539 a maximum of four weeks following rabies virus injection, the injection sites were imaged on a
540 Prairie/Bruker Ultima IV *In Vivo* two-photon microscope driven by a Spectra Physics Mai-Tai Deep
541 See laser with a mode locked Ti:sapphire laser emitting at a wavelength of 1020 nm for tdTomato
542 and mCherry or 920 nm for EGFP. Mice were reanesthetized and mounted via their headplates
543 to a custom frame, again with ointment applied to protect their eyes and with a handwarmer
544 maintaining body temperature. One field of view was chosen in each mouse in the area of maximal
545 fluorescent labelling. The imaging parameters were as follows: image size 512 X 512 pixels (282.6
546 $\mu\text{m} \times 282.6 \mu\text{m}$), 0.782 Hz frame rate, dwell time 4.0 μs , 2x optical zoom, Z-stack step size 1 μm .
547 Image acquisition was controlled with Prairie View 5.4 software. Laser power exiting the 20x
548 water-immersion objective (Zeiss, W plan-apochromat, NA 1.0) varied between 20 and 65 mW
549 depending on focal plane depth (Pockel cell value was automatically increased from 450 at the
550 top section of each stack to 750 at the bottom section). For the example images of labeled cells,
551 maximum intensity projections (stacks of 150-400 μm) were made with Fiji software. Cell counting
552 was performed with the ImageJ Cell Counter plugin. When doing cell counting, week 1 tdTomato
553 labelled cells were defined as a reference; remaining week 1 cells were the same cells at later
554 time point that align with week 1 reference cells but the not-visible cells at week 1 (the dead cells).
555 Plots of cell counts were made with Origin 7.0 software (OriginLab, Northampton, MA). For the
556 thresholded version of this analysis (Supplementary Figure S2), in order to exclude cells that
557 could possibly have been labeled only with mCherry in the SiR-CRE group, only cells with

558 fluorescence intensity greater than the average of the mean red fluorescence intensities of cells
559 imaged in Ai35 versus Ai14 mice at the same laser power at 1020 nm at 7 days postinjection
560 (32.33 a.u.) were included in the population of cells tracked from 7 days onward.

561

562 **Sanger sequencing**

563 RNA viral genomes were extracted from two Tripodi lab (EnvA/ SiR-CRE and EnvA/Sir-FLPo) and
564 one Wickersham lab (RV Δ G-4mCherry) rabies virus samples using a Nucleospin RNA kit
565 (Macherey-Nagel, Germany) and treated with DNase I (37°C for 1 hour, followed by 70°C for 5
566 minutes). Extracted RNA genomes were converted to complementary DNA using an AccuScript
567 PfuUltra II RT-PCR kit (Agilent Technologies, USA) at 42°C for 2 hours with the following
568 barcoded primer annealing to the rabies virus leader sequence:

569 Adapter_N8_leader_fp: TCAGACGATGCGTCATGCNNNNNNNACGCTTAACAACCAGATC

570

571 cDNA sequences from the leader through the first half of the rabies virus P gene were amplified
572 using Platinum SuperFi Green Master Mix (Invitrogen (Thermo Fisher), USA) with cycling
573 conditions as follows: denaturation at 98°C for 30 seconds, followed by 25 cycles of amplification
574 (denaturation at 98°C for 5 seconds and extension at 72°C for 75 seconds), with a final extension
575 at 72°C for 5 minutes, using the following primers:

576 pEX_adapter_fp: CAGCTCAGACGATGCGTCATGC

577 Barcode2_P_rp: GCAGAGTCATGTATAGCTTCTTGAGCTCTCGGCCAG

578

579 The ~2kb PCR amplicons were extracted from an agarose gel, purified with Nucleospin Gel and
580 PCR Clean-up (Macherey-Nagel, Germany), and cloned into pEX-A (Eurofins Genomics, USA)
581 using an In-Fusion HD Cloning Kit (Takara Bio, Japan). The cloned plasmids were transformed
582 into Stellar competent cells (Takara Bio, Japan), and 200 clones per rabies virus sample were
583 isolated and purified for sequencing. For each clone, the index and the 3' end of the N gene were
584 sequenced until sequencing data was collected for over fifty clones per sample: 51 clones from
585 SiR-CRE(EnvA), 50 from SiR-FLPo(EnvA), and 51 from RV Δ G-4mCherry(EnvA). Although viral
586 samples may contain plasmid DNA, viral mRNA, and positive-sense anti-genomic RNA, this RT-
587 PCR procedure can amplify only the negative-sense RNA genome: the reverse transcription
588 primer is designed to anneal to the leader sequence of the negative-strand genome so that cDNA
589 synthesis can start from the negative-sense RNA genome, with no other possible templates.
590 Additionally, the PCR amplifies the cDNA, not any plasmids which were transfected into producer
591 cell lines during viral vector production, because the forward PCR primer anneals to the primer
592 used in the reverse transcription, rather than any viral sequence. This RT-PCR protocol ensures
593 that only negative-sense RNA rabies viral genomes can be sequenced.

594

595 **Sanger sequencing of transgenes in SiR viruses**

596 The procedure for sequencing the transgene inserts was the same as above, but with the RT
597 primer being Adaptor_N8_M_fp (see below), annealing to the M gene and again with a random
598 8-nucleotide index to tag each clone, and with PCR primers pEX_adapter_fp (see above) and
599 Barcode2_L_rp (see below), to amplify the sequences from the 3' end of the M gene to the 5' end
600 of the L gene, covering the iCre-P2A-mCherryPEST (or FLPo-P2A-mCherryPEST) sequence.

601

602 Primers for RT and PCR for Sanger sequencing were as follows:

603 Adaptor_N8_M_fp:

604 TCAGACGATGCGTCATGCNNNNNNNNCAACTCCAACCCTTGGGAGCA

605 Barcode2_L_rp:

606 GCAGAGTCATGTATAGTTGGGGACAATGGGGGTTCC

607

608 **Sanger sequencing analysis**

609 Alignment and mutation detection were performed using SnapGene 4.1.9 (GSL Biotech LLC,
610 USA). Reference sequences of the viral samples used in this study were based on deposited
611 plasmids in Addgene: pSAD-F3-NPEST-iCRE-2A-mCherryPEST (Addgene #99608), pSAD-F3-
612 NPEST-FLPo-2A-mCherryPEST (Addgene #99609), and pRV Δ G-4mCherry (Addgene #52488).
613 Traces corresponding to indices and mutations listed in Figure 1 and Supplementary File S2 were
614 also manually inspected and confirmed.

615

616 **Single-molecule, real-time (SMRT) sequencing**

617 Double-stranded DNA samples for SMRT sequencing were prepared similarly to the above,
618 except that that the clones generated from each of the three virus samples were tagged with one
619 of the standard PacBio barcode sequences to allow identification of each clone's sample of origin
620 following multiplex sequencing (see [https://www.pacb.com/wp-content/uploads/multiplex-target-
621 enrichment-barcoded-multi-kilobase-fragments-probe-based-capture-technologies.pdf](https://www.pacb.com/wp-content/uploads/multiplex-target-enrichment-barcoded-multi-kilobase-fragments-probe-based-capture-technologies.pdf) and
622 [https://github.com/PacificBiosciences/Bioinformatics-Training/wiki/Barcoding-with-SMRT-
623 Analysis-2.3](https://github.com/PacificBiosciences/Bioinformatics-Training/wiki/Barcoding-with-SMRT-Analysis-2.3)). This was in addition to the random index (10 nucleotides in this case) that was
624 again included in the RT primers in order to uniquely tag each individual genome.

625

626 RNA viral genomes were extracted from two Tripodi lab (SiR-CRE and Sir-FLPo) and one
627 Wickersham lab (RV Δ G-4Cre (6); see Addgene #98034 for reference sequence) virus samples
628 using a Nucleospin RNA kit (Macherey-Nagel, Germany) and treated with DNase I (37°C for 1
629 hour, followed by 70° for 5 minutes). Primers for RT and PCR are listed below. PCR cycling
630 conditions were as follows: denaturation at 98°C for 30 seconds, followed by 20 cycles of
631 amplification (denaturation at 98°C for 5 seconds and extension at 72°C for 75 seconds), with a
632 final extension at 72°C for 5 minutes. This left each amplicon with a 16bp barcode at each of its
633 ends that indicated which virus sample it was derived from, in addition to a 10-nt index sequence
634 that was unique to each genome molecule.

635

636 Primers for RT and PCR for SMRT sequencing were as follows:

637 RV Δ G-4Cre:

638 RT:

639 Barcode1_cagc_N10_leader_fp:

640 TCAGACGATGCGTCATCAGCNNNNNNNNNACGCTTAACAACCCAGATC

641 PCR:

642 Barcode1_cagc_fp: TCAGACGATGCGTCAT-CAGC

643 Barcode2_P_rp (see above)

644

645 SiR-CRE:

646 RT:

647 Barcode5_cagc_N10_leader_fp:

648 ACACGCATGACACACTCAGCNNNNNNNNNACGCTTAACAACCCAGATC

649 PCR:

650 Barcode5_cagc_fp: ACACGCATGACACACT-CAGC

651 Barcode3_P_rp: GAGTGCTACTCTAGTACTTCTTGAGCTCTCGGCCAG

652

653 SiR-FLPo:

654 RT:

655 Barcode9_cagc_N10_leader_fp:

656 CTGCGTGCTCTACGACCAGCNNNNNNNNNACGCTTAACAACCCAGATC

657 PCR:

658 Barcode9_cagc_fp: CTGCGTGCTCTACGAC-CAGC

659 Barcode4_P_rp: CATGTAAGTATACACACTTCTTGAGCTCTCGGCCAG

660
661
662
663
664
665
666
667
668

After the amplicons were extracted and purified from an agarose gel, the three were mixed together at 1:1:1 molar ratio. The amplicons' sizes were confirmed on the Fragment Analyzer (Agilent Technologies, USA), then hairpin loops were ligated to both ends of the mixed amplicons to make circular SMRTbell templates for PacBio Sequel sequencing. SMRTbell library preparation used the PacBio Template Preparation Kit v1.0 and Sequel Chemistry v3. Samples were then sequenced on a PacBio Sequel system running Sequel System v.6.0 (Pacific Biosciences, USA), with a 10-hour movie time.

669 **Bioinformatics for PacBio sequence analysis**

670 For the ~2kb template, the DNA polymerase with a strand displacement function can circle around
671 the template and hairpins multiple times; the consensus sequence of multiple passes yields a
672 CCS (circular consensus sequence) read for each molecule. Raw sequences were initially
673 processed using SMRT Link v.6.0 (Pacific Biosciences, USA). Sequences were filtered for a
674 minimum of read length 10 bp, pass 3, and read score 65. 127,178 CCS reads were filtered
675 through passes 3 and Q10; 89,188 CCS reads through passes 5 and Q20; 29,924 CCS reads
676 through passes 8 and Q30. Downstream bioinformatics analysis was performed using BLASR
677 V5.3.2 for the alignment, bcftools v.1.6 for variant calling. Mutations listed in Figure 2 and
678 Supplementary File S3 were also manually inspected and confirmed using Integrative Genomics
679 Viewer 2.3.32 (software.broadinstitute.org/software/igv/). Analysis steps included the following: 1.
680 Exclude CCS reads under 1000 bases, which may have been derived from non-specific reverse
681 transcription or PCR reactions. 2. Classify the CCS reads to the three samples, according to the
682 PacBio barcodes on the 5' ends. 3. For any CCS reads that contain the same 10-nucleotide
683 random index, select only one of them, to avoid double-counting of clones derived from the same
684 cDNA molecule. 4. Align the reads to the corresponding reference sequence (see Supplementary
685 Files S4-S6). 5. Count the number of mutations at each nucleotide position of the reference
686 sequences.

687
688

689 **ACKNOWLEDGEMENTS**

690 We thank Ernesto Ciabatti and Marco Tripodi for sharing samples of EnvA/SiR-CRE and
691 EnvA/SiR-FLPo and for comments on the manuscript. We thank Sean Whelan and Ayano
692 Matsushima for helpful discussion and Jun Zhuang, Soumya Chatterjee, and Ali Cetin for helpful
693 discussion and sharing their own results. We thank Stuart Levine, Noelani Kamelamela, and
694 Huiming Ding of the MIT BioMicro Center for assistance with SMRT sequencing and bioinformatic
695 data analysis. Research reported in this publication was supported by BRAIN Initiative awards
696 U01MH106018 (Wickersham), U01MH114829 (Dong), and U19MH114830 (Zeng) from the
697 National Institute of Mental Health.

698
699

700 **FIGURE LEGENDS**

701 *Legends here are for the main figures only. Legends for Supplementary Information are after*
702 *the main figure images below.*

703
704

705 **Figure 1: Single-molecule Sanger sequencing of barcoded viral genomes reveals that most** 706 **SiR virions have lost the intended C-terminal modification to the nucleoprotein.**

707 (A) Schematic of the RT-PCR workflow. In the reverse transcription (RT) step, the RT primer,
708 containing a random 8-nucleotide sequence, anneals to the 3' rabies virus leader, adding a unique
709 random index to the 5' end of the cDNA molecule corresponding to each individual viral particle's
710 RNA genome. In the PCR step, the forward PCR primer anneals to the RT primer sequence and

711 the reverse PCR primer anneals within the viral phosphoprotein gene P. Both PCR primers have
712 15-base sequences homologous to those flanking an insertion site in a plasmid used for
713 sequencing, allowing the amplicons to be cloned into the plasmid using a seamless cloning
714 method before transformation into bacteria. The resulting plasmid library consists of plasmids
715 containing up to 4^8 different index sequences, allowing confirmation that the sequences of
716 plasmids purified from individual picked colonies correspond to the sequences of different
717 individual rabies viral particles' genomes.

718 (B) Representative Sanger sequencing data of the 8-bp index and the TEV-PEST sequence.
719 Mutations are highlighted in red.

720 (C) Mutation variants and their frequencies in each viral vector sample based on Sanger
721 sequencing data. No unmutated genomes were found in the SiR-CRE sample: 50 out of 51 had
722 a substitution creating an opal stop codon just before the TEV cleavage site, and the 51st genome
723 contained a frameshift which also removed the C-terminal addition. In the SiR-FLPo sample, only
724 4 out of 50 clones had an intact sequence of the C-terminal addition; the other 46 out of 50 had
725 one of two *de novo* stop codons at the end of N or the beginning of the TEV cleavage site. In the
726 sample of RV Δ G-4mCherry, a virus from our laboratory included as a control to distinguish true
727 mutations on the rabies genomes from mutations due to the RT-PCR process, none of the 51
728 clones analyzed had mutations in the sequenced region.

729

730 **Figure 2: Single-molecule, real-time (SMRT) sequencing of thousands of barcoded viral**
731 **genomes confirms that most SiR virions have lost the intended C-terminal modification to**
732 **the nucleoprotein.**

733 (A) Schematic of workflow for SMRT sequencing. An RT primer with a random 10-nucleotide
734 sequence anneals to the leader sequence on the negative-sense single-stranded RNA genome.
735 Forward and reverse PCR primers have distinct SMRT barcodes at their 5' ends for the three
736 different virus samples. After RT-PCR, each amplicon library consists of amplicons each
737 containing a SMRT barcode to identify the sample of origin as well as the 10-nucleotide index
738 (i.e., with a potential diversity of 4^{10} different indices) to uniquely label the individual genome of
739 origin. SMRT "dumbbell" adaptors are then ligated to the amplicons' ends, making circular
740 templates which are then repeatedly traversed by a DNA polymerase, resulting in long
741 polymerase reads each containing multiple reads of the positive and negative strands. The
742 individual subreads for a given molecule are combined to form circular consensus sequence
743 (CCS) reads.

744 (B) High-frequency (>2%) point mutations found in the rabies vector samples based on SMRT
745 sequencing. Horizontal axis represents nucleotide position along the reference sequences (see
746 text); vertical axis represents variant frequency. Total number of CCS3 reads (i.e., with at least 3
747 subreads for each position) are 22,205 for SiR-CRE, 17,086 reads for SiR-FLPo, and 17,978
748 reads for RV Δ G-4Cre. The great majority of SiR-CRE and SiR-FLPo genomes have point
749 mutations creating premature stop codons at or just after the end of N and before the C-terminal
750 addition. The only frequent (>2%) mutation found in the control virus, RV Δ G-4Cre, was a single
751 amino acid substitution at position 419 in 9.49% of virions. Insertions and deletions are not shown
752 here (see text).

753 (C) Summary of results. In the SiR virus samples, 99.22% of SiR-Cre virions and 83.85% of SiR-
754 FLPo virions had point mutations creating premature stop codons that completely removed the
755 intended C-terminal addition to the nucleoprotein, making them simply first-generation (Δ G) rabies
756 viral vectors. This does not include any insertions or deletions causing frameshifts (see text),
757 which would further increase the percentage of first-generation-type virions in these samples. In
758 the RV Δ G-4Cre sample, there were no premature stop codons at or near the end of the
759 nucleoprotein gene.

760

761 **Figure 3: SiR viruses appear to cause expression of viral nucleoprotein at levels similar to**
762 **those of first-generation ΔG viruses.**

763 (A-D) Reporter cells infected with first-generation, ΔG viruses show characteristic bright, clumpy
764 anti-nucleoprotein staining (green), indicating high nucleoprotein expression and active viral
765 replication. Red is mCherry expression, reporting expression of Cre or FLPO; blue is mTagBFP2,
766 constitutively expressed by these reporter cell lines.

767 (E-H) Reporter cells infected with second-generation, ΔGL viruses show only punctate staining
768 for nucleoprotein, indicating isolated individual viral particles or ribonucleoprotein complexes;
769 these viruses do not replicate intracellularly (6). Reporter cassette activation takes longer from
770 the lower recombinase expression levels of these viruses, so mCherry expression is dimmer than
771 in cells infected with ΔG viruses at the same time point.

772 (I-J) Reporter cells infected with SiR viruses show clumps of nucleoprotein and rapid reporter
773 expression indicating high expression of recombinases, similarly to cells infected with ΔG viruses.
774 Scale bar: 100 μm , applies to all panels.

775
776 **Figure 4: Longitudinal two-photon imaging *in vivo* shows that SiR virus kills approximately**
777 **80% of infected neurons *in vivo* within 2-4 weeks.**

778 A) Representative fields of view (FOVs) of visual cortical neurons labeled with RV ΔG -4Cre (top
779 row), RV ΔGL -4Cre (middle row), or SiR-CRE (bottom row) in Ai14 mice (Cre-dependent
780 expression of tdTomato). Images within each row are of the same FOV imaged at the four different
781 time points in the same mouse. Circles indicate cells that are present at 7 days postinjection but
782 no longer visible at a subsequent time point. Scale bar: 50 μm , applies to all images.

783 B-D) Numbers of cells present at week 1 that were still present in subsequent weeks. While very
784 few cells labeled with RV ΔGL -4Cre were lost, and RV ΔG -4Cre killed a significant minority of cells,
785 SiR-CRE killed the majority of labeled neurons within 14 days following injection.

786 E) Percentages of cells present at week 1 that were still present in subsequent imaging sessions.
787 By 28 days postinjection, an average of only 20.5% of cells labeled by SiR-CRE remained.

788
789 **Figure 5: 86% of SiR-CRE-labeled neurons in Arch-EGFP-ER2 reporter mice disappear**
790 **between 11 days and 28 days after injection.**

791 A) Maximum intensity projections of the two-photon FOV shown in Supplementary Video S1 of
792 visual cortical neurons labeled with SiR-CRE in an Ai35 mouse, 11-28 days postinjection. Images
793 are from the same FOV at four different time points. All cells clearly visible on day 11 are circled.
794 In this example, 18 out of 19 cells (red circles) disappeared by a subsequent imaging session.
795 Only one cell (white circle) is still visible on day 28. Numbers below four of the circles mark the
796 cells for which intensity profiles are shown in panel B. Scale bar: 50 μm , applies to all images.

797 B) Green fluorescence intensity versus depth for the four representative neurons numbered in
798 panel A at the four different time points, showing disappearance of three of them over time.

799 C) Fraction of cells visibly EGFP-labeled at day 11 still visible at later time points, from four
800 different FOVs in two Ai35 mice. Connected sets of markers indicate cells from the same FOV.
801 86% of SiR-CRE-labeled neurons had disappeared by 4 weeks postinjection.

802
803
804 **LEGENDS FOR SUPPLEMENTARY INFORMATION**

805
806 **Supplementary File S1: >90% of SiR-CRE viral particles with the mCherry gene intact also**
807 **have the Cre gene intact, suggesting that most of the SiR-CRE-infected cells that**
808 **disappear over time in tdTomato reporter mice are dying rather than simply stopping**
809 **expression of mCherry.**

810 We sequenced the transgene inserts for 21 individual SiR-CRE clones (see Methods). 19 out of
811 21 had no mutations in the Cre gene, and two had one point mutation each (Ala88Val and

812 Arg189Ile). All 21 had an intact mCherry gene. The lack of a large proportion of Cre-knockout
813 mutants is one indication that the majority of red fluorescent neurons in SiR-CRE-injected Ai14
814 (tdTomato reporter) mice are not labeled only with mCherry, providing evidence that their
815 disappearance is equivalent to their death. Parenthetically, we also partially sequenced the
816 transgene insert for four individual clones of the SiR-FLPo sample, just to confirm the identity of
817 the virus. In one of the four sequenced virions, we found a 15 bp deletion in the FLPo gene as
818 well as a synonymous Thr -> Thr (ACC -> ACA) substitution at position 47 of the mCherry gene;
819 in another, we found a Gly -> Ser mutation at position 4 of the mCherry gene. We did not find
820 mutations in the transgenes of other two SiR-FLPo genomes sequenced (data not shown).

821

822 **Supplementary Figure S1: mCherry fluorescence from SiR-CRE is much dimmer than**
823 **tdTomato fluorescence in Ai14 mice, suggesting that the disappearance of the brighter**
824 **cells in SiR-CRE-injected Ai14 mice indicates their death.**

825 A) Representative images of red fluorescence in SiR-CRE-labeled cells in Ai14 (Cre-dependent
826 expression of tdTomato, top row) and Ai35 (Cre-dependent expression of Arch-EGFP-ER2,
827 bottom row). The three images for each mouse line are from 3 different mice of each line, imaged
828 7 days following SiR-CRE injection (see Methods), all with the same laser intensity and
829 wavelength (1020 nm). Red fluorescence due only to mCherry (i.e., in Ai35 mice) is obviously
830 much dimmer than that due to tdTomato (i.e., in Ai14 mice). Scale bar: 50 μ m, applies to all
831 images.

832 B) Intensity of red fluorescence of SiR-CRE-labeled cells in Ai14 (left) and Ai35 (right) mice. Data
833 point indicate intensity of individual cells in arbitrary units at the same laser and microscope
834 settings (see Methods). Box plots indicate median, 25th–75th percentiles (boxes), and full range
835 (whiskers) of intensities for each mouse. The average of the mean red fluorescent intensity in
836 each mouse was 48.97 in Ai14 and 15.69 in Ai35 ($p=0.00283 < 0.01$, one-way ANOVA); the
837 midpoint of these means, 32.33, was used as the cutoff for the reanalysis of the data in Ai14 mice
838 to exclude neurons that could have been labeled with mCherry alone.

839

840 **Supplementary Video S1: Video of 95% of SiR-CRE-labeled neurons in an Arch-EGFP-ER2**
841 **reporter mouse disappearing between 11 days and 28 days postinjection.**

842 Two-photon image stacks of a single FOV of visual cortical neurons in an Ai35 mouse imaged at
843 four different time points; time in the video represents depth of focus. Large blobs are glia. 18 out
844 of the 19 neurons visibly labeled with Arch-EGFP-ER2 at 11 days following injection of SiR-Cre
845 are no longer visible 17 days later. White circles indicate cells present at both 11 days and all
846 subsequent imaging sessions; red circles indicate cells present at 11 days but gone by 28 days.

847

848 **Supplementary Figure S2: 81% of SiR-CRE-labeled neurons in tdTomato reporter mice**
849 **disappear within 2-4 weeks, even excluding dimmer cells that might have only been labeled**
850 **with mCherry.**

851 A) Same representative fields of view as in Figure 4 but with circles now marking only cells with
852 intensity at 7 days of greater than 32.33 a.u. (see text and Supplementary Figure S1) that are no
853 longer visible at a subsequent time point. Scale bar: 50 μ m, applies to all images.

854 B-D) Numbers of cells above threshold fluorescence intensity at week 1 that were still present in
855 subsequent weeks. The conclusions from Figure 4 are unchanged: few cells labeled with RV Δ GL-
856 4Cre were lost, RV Δ G-4Cre killed a significant minority of cells, and SiR-CRE killed the majority
857 of labeled neurons within two weeks following injection.

858 E) Percentages of cells above threshold at week 1 that were still present in subsequent imaging
859 sessions. By 28 days postinjection, an average of only 19.2% of suprathreshold SiR-CRE-labeled
860 cells remained.

861

862 **Supplementary File S2: Sanger sequencing data of all clones shown in Figure 1.**

863 51 clones derived from SiR-CRE, 50 from SiR-FLPo, and 51 from RV Δ G-4mCherry are identified
864 by their unique indices. All of the indices as well as the sequences corresponding to the 3' end of
865 the nucleoprotein gene are shown.

866

867 **Supplementary File S3: Summary tables of SMRT sequencing data.** These tables show all
868 mutations occurring at positions mutated at greater than 2% frequency in the three virus
869 samples analyzed. Position numbers in these tables refer to the sequences in the three
870 Genbank files below (Supplementary Files S4-S5).

871

872 **Supplementary File S4: SiR-CRE amplicon reference sequence.** This Genbank-format file
873 contains the expected (i.e., based on the published sequence: Addgene #99608) sequence of
874 amplicons obtained from SiR-CRE for SMRT sequencing.

875

876 **Supplementary File S5: SiR-FLPo amplicon reference sequence.** This Genbank-format file
877 contains the expected (i.e., based on the published sequence: Addgene # 99609) sequence of
878 amplicons obtained from SiR-FLPo for SMRT sequencing.

879

880 **Supplementary File S6: RV Δ G-4Cre amplicon reference sequence.** This Genbank-format file
881 contains the expected (i.e., based on the published sequence: see Addgene #98034) sequence
882 of amplicons obtained from RV Δ G-4Cre for SMRT sequencing.

883

884 **Supplementary Figure S3: First-generation vector RV Δ G-4FLPo appears to be toxic to**
885 **most cells, unlike the comparable first-generation vector RV Δ G-Cre.** Although we did not
886 rigorously quantify the effect, our FLPo-encoding RV Δ G-4FLPo appears to kill neurons more
887 quickly than does RV Δ G-4Cre (cf. Figure 4 and Chatterjee et al. (6)). In this example field of
888 view, most neurons clearly visible at earlier time points have disappeared by 28 days
889 postinjection, leaving degenerating cellular debris. See Discussion for possible reasons why a
890 preparation of a first-generation vector encoding a recombinase may or may not preserve a
891 large percentage of infected neurons. Scale bar: 50 μ m, applies to all panels.

892

893

894 REFERENCES

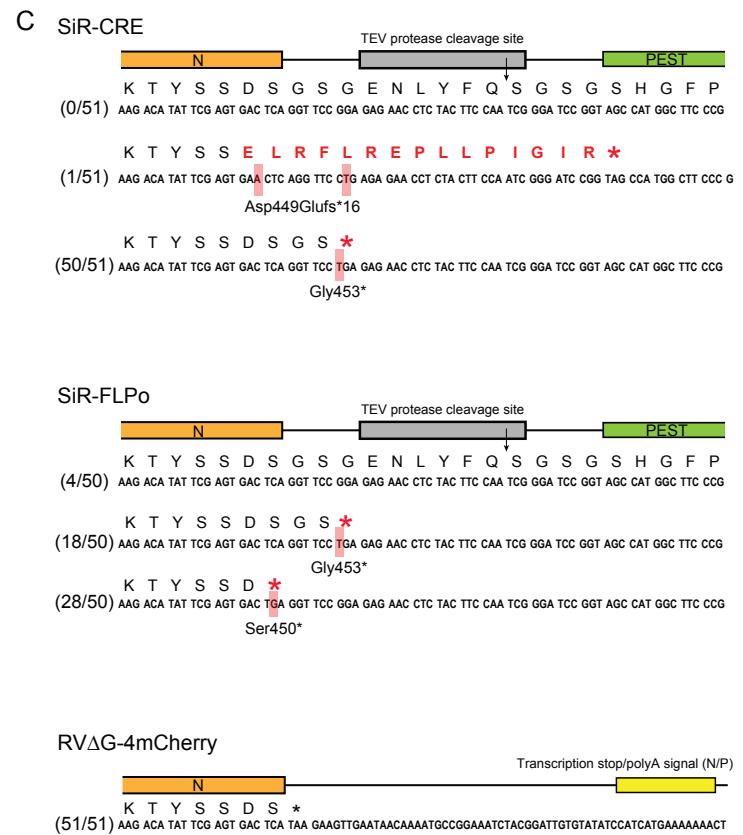
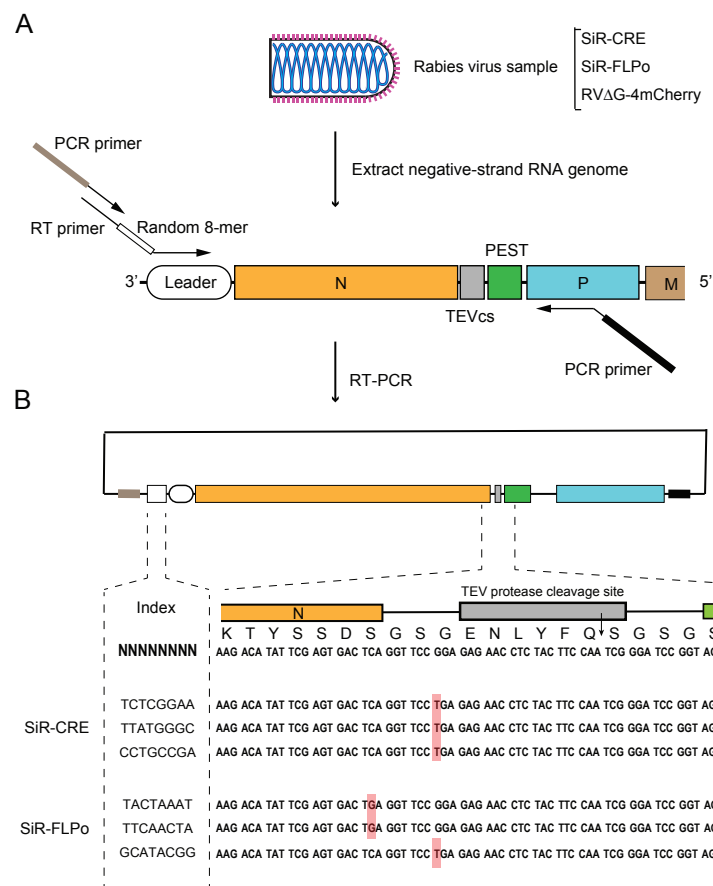
895

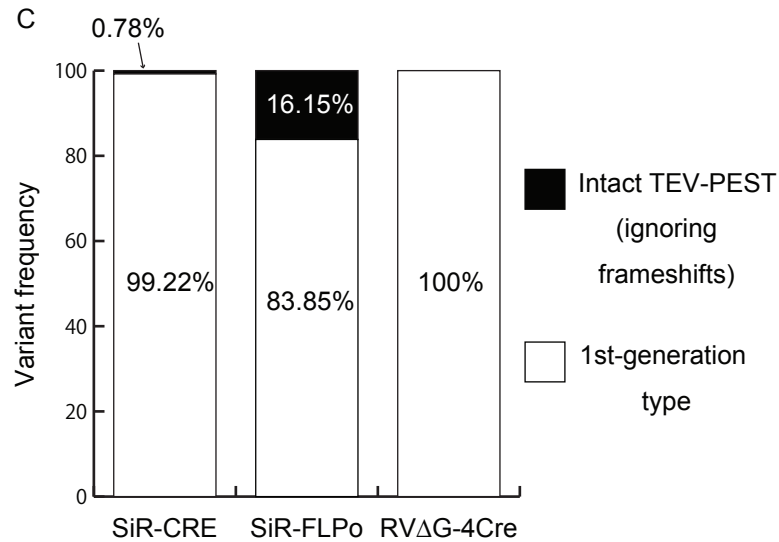
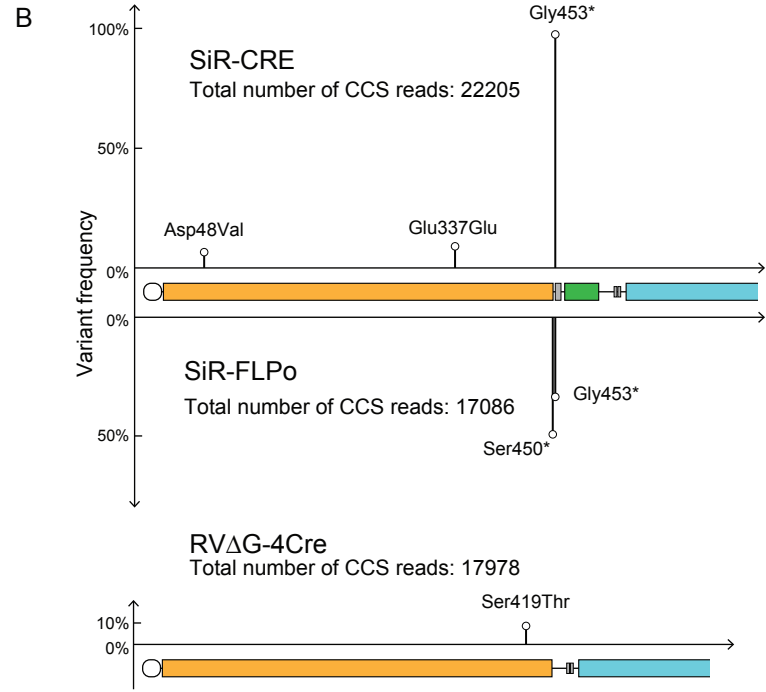
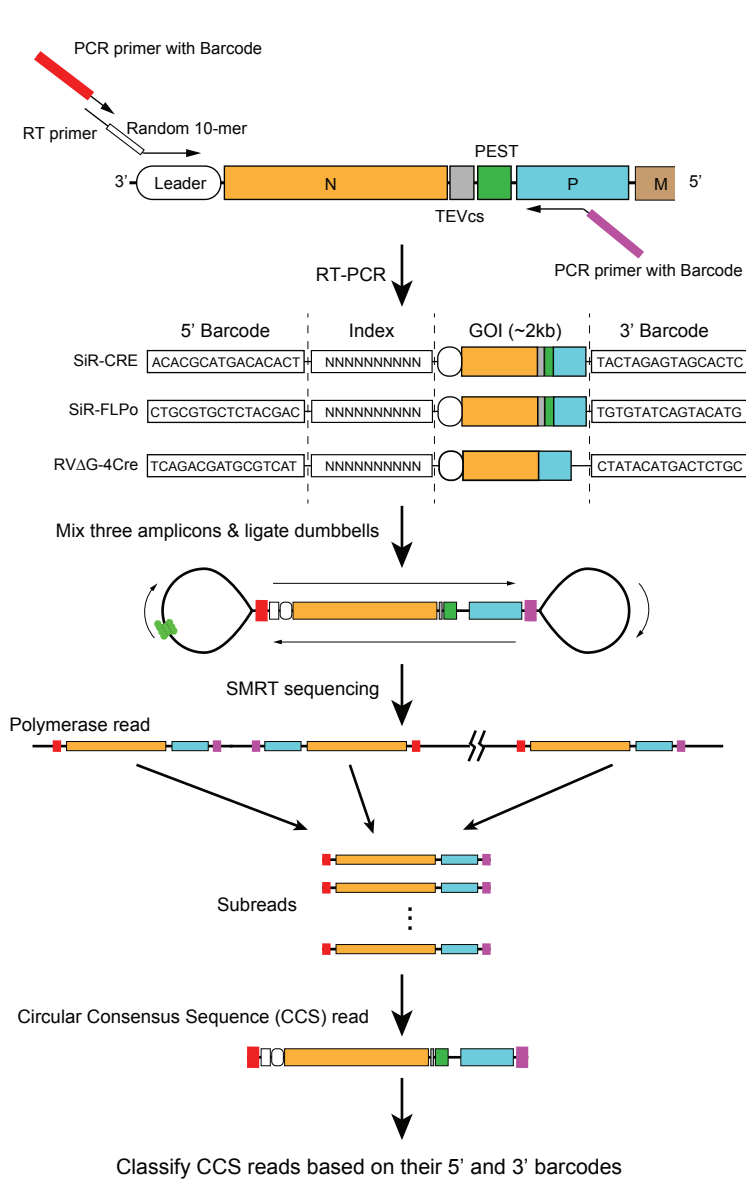
- 896 1. Wickersham IR, et al. (2007) Monosynaptic restriction of transsynaptic tracing from
897 single, genetically targeted neurons. *Neuron* 53(5):639-647.
- 898 2. Augustine V, et al. (2018) Hierarchical neural architecture underlying thirst regulation.
899 *Nature* 555(7695):204-209.
- 900 3. Kohl J, et al. (2018) Functional circuit architecture underlying parental behaviour. *Nature*
901 556(7701):326-331.
- 902 4. Evans DA, et al. (2018) A synaptic threshold mechanism for computing escape
903 decisions. *Nature* 558(7711):590-594.
- 904 5. Kaelberer MM, et al. (2018) A gut-brain neural circuit for nutrient sensory transduction.
905 *Science* 361(6408).
- 906 6. Chatterjee S, et al. (2018) Nontoxic, double-deletion-mutant rabies viral vectors for
907 retrograde targeting of projection neurons. *Nat Neurosci* 21(4):638-646.
- 908 7. Wickersham IR, Finke S, Conzelmann KK, & Callaway EM (2007) Retrograde neuronal
909 tracing with a deletion-mutant rabies virus. *Nature Methods* 4(1):47-49.
- 910 8. Reardon TR, et al. (2016) Rabies Virus CVS-N2c(DeltaG) Strain Enhances Retrograde
911 Synaptic Transfer and Neuronal Viability. *Neuron* 89(4):711-724.

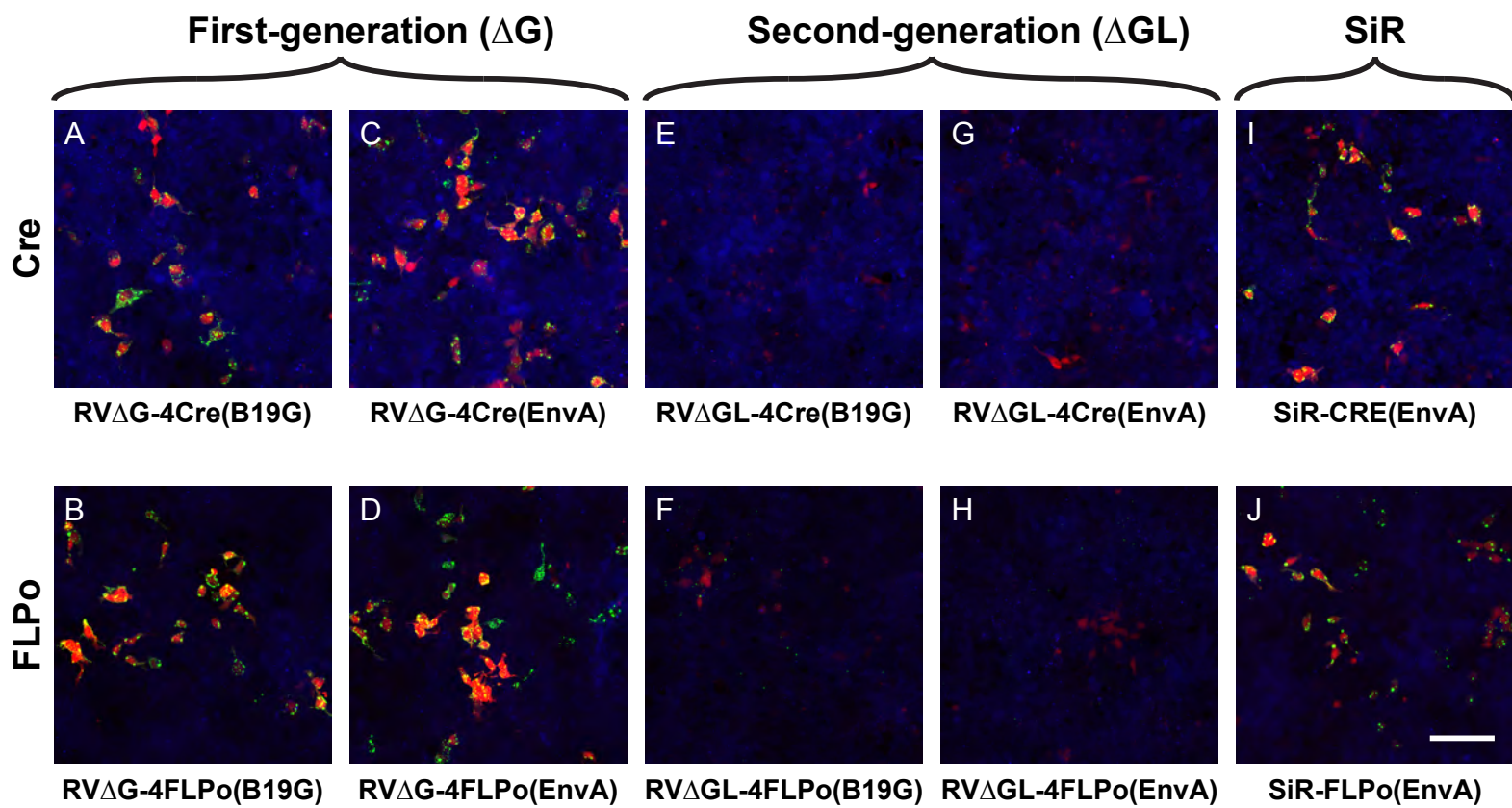
- 912 9. Morimoto K, Hooper DC, Spitsin S, Koprowski H, & Dietzschold B (1999) Pathogenicity
913 of different rabies virus variants inversely correlates with apoptosis and rabies virus
914 glycoprotein expression in infected primary neuron cultures. *J Virol* 73(1):510-518.
- 915 10. Ciabatti E, Gonzalez-Rueda A, Mariotti L, Morgese F, & Tripodi M (2017) Life-Long
916 Genetic and Functional Access to Neural Circuits Using Self-Inactivating Rabies Virus.
917 *Cell* 170(2):382-392 e314.
- 918 11. Steinhauer DA & Holland JJ (1987) Rapid evolution of RNA viruses. *Annu Rev Microbiol*
919 41:409-433.
- 920 12. Steinhauer DA, de la Torre JC, & Holland JJ (1989) High nucleotide substitution error
921 frequencies in clonal pools of vesicular stomatitis virus. *J Virol* 63(5):2063-2071.
- 922 13. Holland JJ, De La Torre JC, & Steinhauer DA (1992) RNA virus populations as
923 quasispecies. *Curr Top Microbiol Immunol* 176:1-20.
- 924 14. Holmes EC, Woelk CH, Kassis R, & Bourhy H (2002) Genetic constraints and the
925 adaptive evolution of rabies virus in nature. *Virology* 292(2):247-257.
- 926 15. Jenkins GM, Rambaut A, Pybus OG, & Holmes EC (2002) Rates of molecular evolution
927 in RNA viruses: a quantitative phylogenetic analysis. *J Mol Evol* 54(2):156-165.
- 928 16. Combe M & Sanjuan R (2014) Variation in RNA virus mutation rates across host cells.
929 *PLoS Pathog* 10(1):e1003855.
- 930 17. Wickersham IR, Sullivan HA, & Seung HS (2010) Production of glycoprotein-deleted
931 rabies viruses for monosynaptic tracing and high-level gene expression in neurons.
932 *Nature protocols* 5(3):595-606.
- 933 18. Osakada F & Callaway EM (2013) Design and generation of recombinant rabies virus
934 vectors. *Nat Protoc* 8(8):1583-1601.
- 935 19. Wickersham IR & Sullivan HA (2015) Rabies viral vectors for monosynaptic tracing and
936 targeted transgene expression in neurons. *Cold Spring Harb Protoc* 2015(4):375-385.
- 937 20. Weible AP, *et al.* (2010) Transgenic targeting of recombinant rabies virus reveals
938 monosynaptic connectivity of specific neurons. *The Journal of neuroscience : the official*
939 *journal of the Society for Neuroscience* 30(49):16509-16513.
- 940 21. Carneiro MO, *et al.* (2012) Pacific biosciences sequencing technology for genotyping
941 and variation discovery in human data. *BMC Genomics* 13:375.
- 942 22. Wirblich C & Schnell MJ (2011) Rabies virus (RV) glycoprotein expression levels are not
943 critical for pathogenicity of RV. *J Virol* 85(2):697-704.
- 944 23. Tao L, *et al.* (2010) Molecular basis of neurovirulence of flury rabies virus vaccine
945 strains: importance of the polymerase and the glycoprotein R333Q mutation. *J Virol*
946 84(17):8926-8936.
- 947 24. Prehaud C, Lay S, Dietzschold B, & Lafon M (2003) Glycoprotein of nonpathogenic
948 rabies viruses is a key determinant of human cell apoptosis. *J Virol* 77(19):10537-10547.
- 949 25. Madisen L, *et al.* (2012) A toolbox of Cre-dependent optogenetic transgenic mice for
950 light-induced activation and silencing. *Nature neuroscience* 15(5):793-802.
- 951 26. Shaner NC, *et al.* (2004) Improved monomeric red, orange and yellow fluorescent
952 proteins derived from *Discosoma* sp. red fluorescent protein. *Nat Biotechnol*
953 22(12):1567-1572.
- 954 27. Drobizhev M, Makarov NS, Tillo SE, Hughes TE, & Rebane A (2011) Two-photon
955 absorption properties of fluorescent proteins. *Nat Methods* 8(5):393-399.
- 956 28. Huang KW & Sabatini BL (2020) Single-Cell Analysis of Neuroinflammatory Responses
957 Following Intracranial Injection of G-Deleted Rabies Viruses. *Front Cell Neurosci* 14:65.
- 958 29. Prosniak M, Hooper DC, Dietzschold B, & Koprowski H (2001) Effect of rabies virus
959 infection on gene expression in mouse brain. *Proc Natl Acad Sci U S A* 98(5):2758-
960 2763.

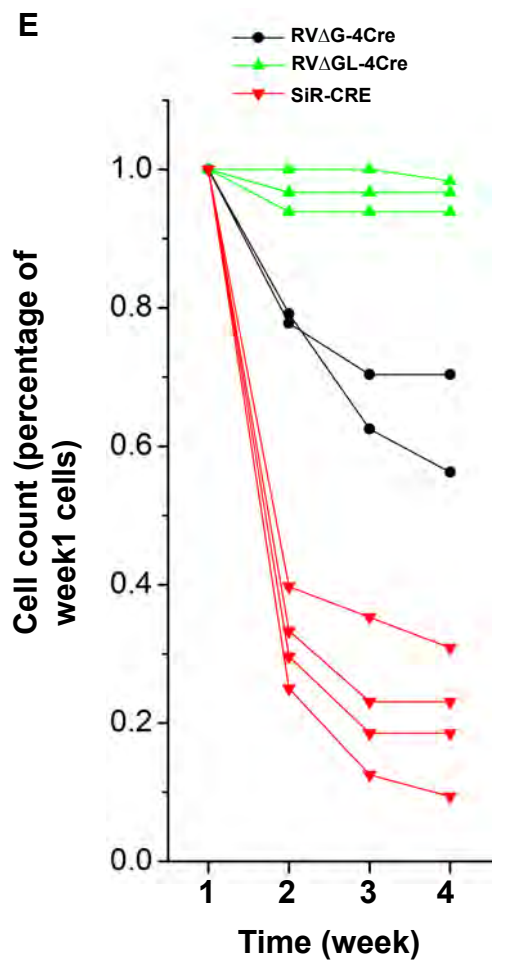
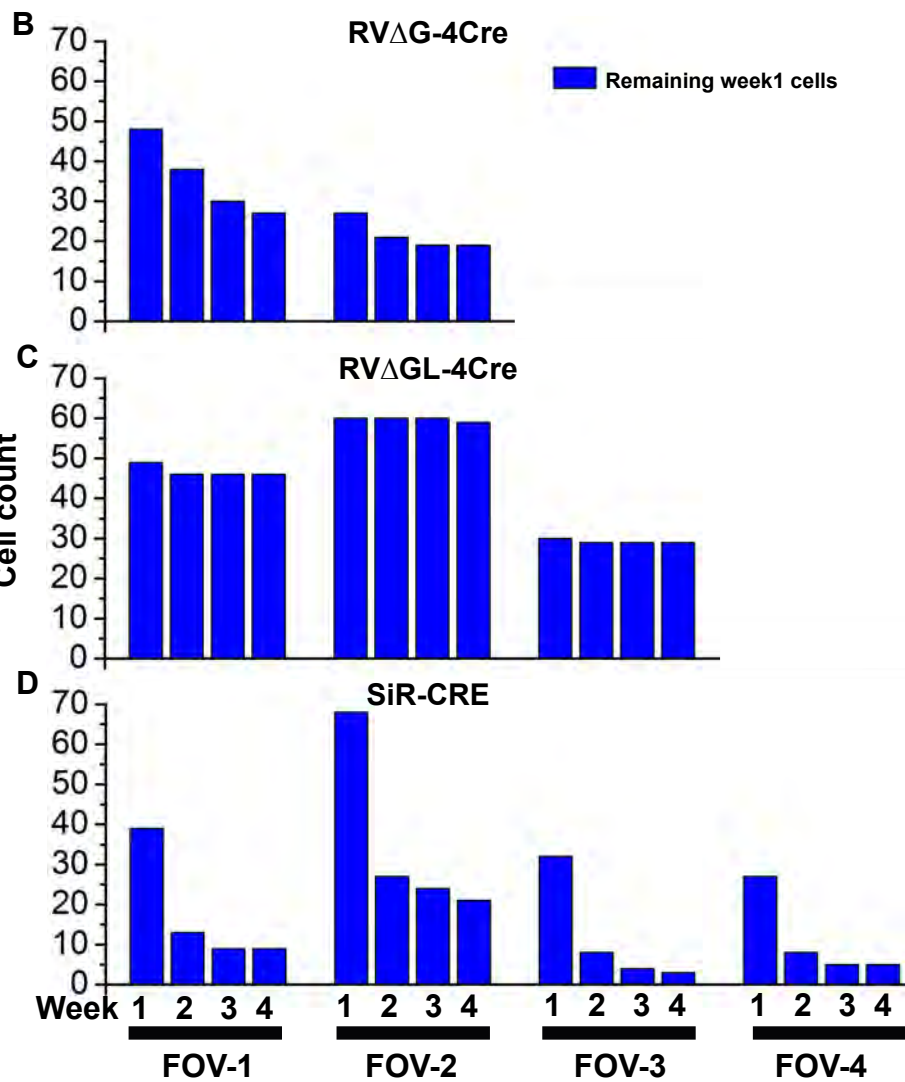
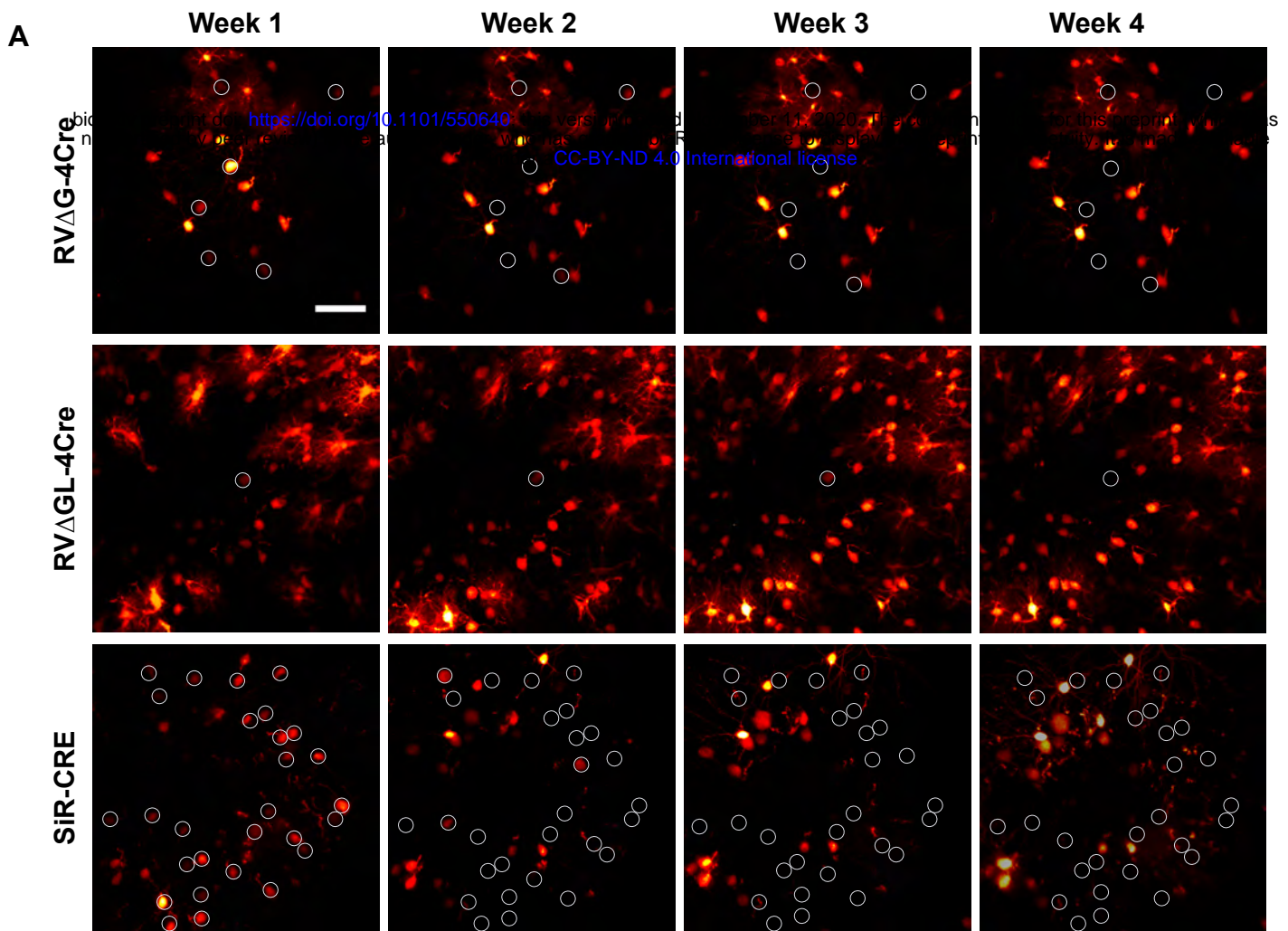
- 961 30. Gomme EA, Wirblich C, Addya S, Rall GF, & Schnell MJ (2012) Immune clearance of
962 attenuated rabies virus results in neuronal survival with altered gene expression. *PLoS*
963 *Pathog* 8(10):e1002971.
- 964 31. Wiktor TJ, Dietzschold B, Leamson RN, & Koprowski H (1977) Induction and biological
965 properties of defective interfering particles of rabies virus. *J Virol* 21(2):626-635.
- 966 32. Kawai A & Matsumoto S (1977) Interfering and noninterfering defective particles
967 generated by a rabies small plaque variant virus. *Virology* 76(1):60-71.
- 968 33. Clark HF, Parks NF, & Wunner WH (1981) Defective interfering particles of fixed rabies
969 viruses: lack of correlation with attenuation or auto-interference in mice. *J Gen Virol*
970 52(Pt 2):245-258.
- 971 34. Dalton KP & Rose JK (2001) Vesicular stomatitis virus glycoprotein containing the entire
972 green fluorescent protein on its cytoplasmic domain is incorporated efficiently into virus
973 particles. *Virology* 279(2):414-421.
- 974 35. Duprex WP, Collins FM, & Rima BK (2002) Modulating the function of the measles virus
975 RNA-dependent RNA polymerase by insertion of green fluorescent protein into the open
976 reading frame. *J Virol* 76(14):7322-7328.
- 977 36. Finke S, Brzozka K, & Conzelmann KK (2004) Tracking fluorescence-labeled rabies
978 virus: enhanced green fluorescent protein-tagged phosphoprotein p supports virus gene
979 expression and formation of infectious particles. *J Virol* 78(22):12333-12343.
- 980 37. Koser ML, *et al.* (2004) Rabies virus nucleoprotein as a carrier for foreign antigens. *Proc*
981 *Natl Acad Sci U S A* 101(25):9405-9410.
- 982 38. Brown DD, *et al.* (2005) Rational attenuation of a morbillivirus by modulating the activity
983 of the RNA-dependent RNA polymerase. *J Virol* 79(22):14330-14338.
- 984 39. Das SC, Nayak D, Zhou Y, & Pattnaik AK (2006) Visualization of intracellular transport of
985 vesicular stomatitis virus nucleocapsids in living cells. *J Virol* 80(13):6368-6377.
- 986 40. Klingen Y, Conzelmann KK, & Finke S (2008) Double-labeled rabies virus: live tracking
987 of enveloped virus transport. *Journal of virology* 82(1):237-245.
- 988 41. Das SC, Panda D, Nayak D, & Pattnaik AK (2009) Biarsenical labeling of vesicular
989 stomatitis virus encoding tetracysteine-tagged m protein allows dynamic imaging of m
990 protein and virus uncoating in infected cells. *J Virol* 83(6):2611-2622.
- 991 42. Marriott AC & Hornsey CA (2011) Reverse genetics system for Chandipura virus:
992 tagging the viral matrix protein with green fluorescent protein. *Virus Res* 160(1-2):166-
993 172.
- 994 43. Soh TK & Whelan SP (2015) Tracking the Fate of Genetically Distinct Vesicular
995 Stomatitis Virus Matrix Proteins Highlights the Role for Late Domains in Assembly. *J*
996 *Virol* 89(23):11750-11760.
- 997 44. Nikolic J, Civas A, Lama Z, Lagaudriere-Gesbert C, & Blondel D (2016) Rabies Virus
998 Infection Induces the Formation of Stress Granules Closely Connected to the Viral
999 Factories. *PLoS Pathog* 12(10):e1005942.
- 1000 45. Case JB, *et al.* (2020) Replication-competent vesicular stomatitis virus vaccine vector
1001 protects against SARS-CoV-2-mediated pathogenesis. *bioRxiv*.
- 1002 46. Matsuyama M, *et al.* (2019) "Self-inactivating" rabies viruses are just first-generation, ΔG
1003 rabies viruses. *bioRxiv*:550640.
- 1004 47. Ciabatti E, *et al.* (2020) Genomic stability of Self-inactivating Rabies.
1005 *bioRxiv*:2020.2009.2019.304683.
- 1006 48. Marr RA, *et al.* (2004) Neprilysin regulates amyloid Beta peptide levels. *J Mol Neurosci*
1007 22(1-2):5-11.
- 1008 49. Niwa H, Yamamura K, & Miyazaki J (1991) Efficient selection for high-expression
1009 transfectants with a novel eukaryotic vector. *Gene* 108(2):193-199.
- 1010 50. Atasoy D, Aponte Y, Su HH, & Sternson SM (2008) A FLEX switch targets
1011 Channelrhodopsin-2 to multiple cell types for imaging and long-range circuit mapping.

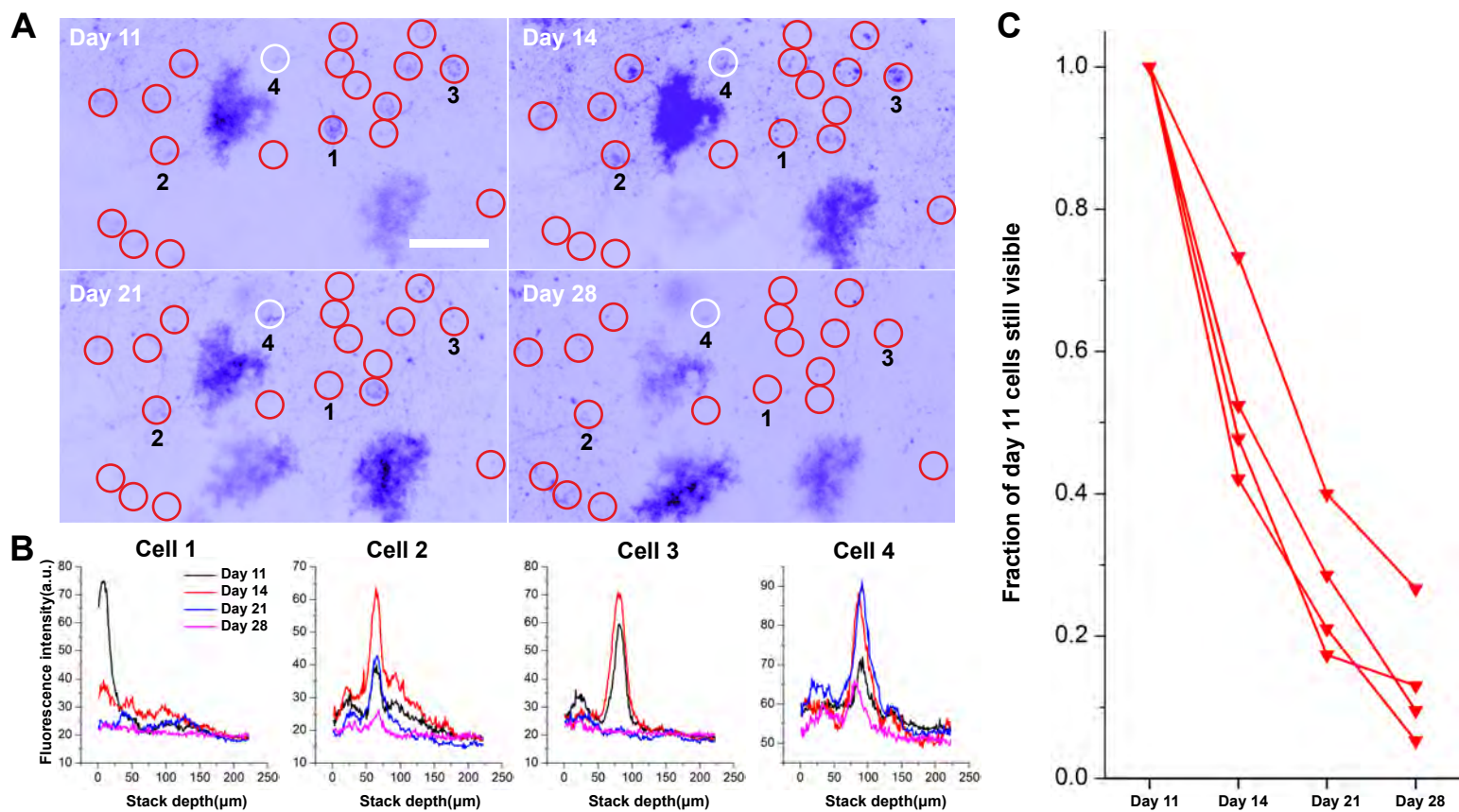
- 1012 *The Journal of neuroscience : the official journal of the Society for Neuroscience*
1013 28(28):7025-7030.
- 1014 51. Subach OM, Cranfill PJ, Davidson MW, & Verkhusha VV (2011) An enhanced
1015 monomeric blue fluorescent protein with the high chemical stability of the chromophore.
1016 *PLoS One* 6(12):e28674.
- 1017 52. Turan S, Kuehle J, Schambach A, Baum C, & Bode J (2010) Multiplexing RMCE:
1018 versatile extensions of the Flp-recombinase-mediated cassette-exchange technology. *J*
1019 *Mol Biol* 402(1):52-69.
- 1020 53. Matsuda T & Cepko CL (2004) Electroporation and RNA interference in the rodent retina
1021 in vivo and in vitro. *P Natl Acad Sci USA* 101(1):16-22.
- 1022 54. Bates P, Young JA, & Varmus HE (1993) A receptor for subgroup A Rous sarcoma virus
1023 is related to the low density lipoprotein receptor. *Cell* 74(6):1043-1051.
- 1024 55. Raymond CS & Soriano P (2007) High-efficiency FLP and PhiC31 site-specific
1025 recombination in mammalian cells. *PLoS One* 2(1):e162.
- 1026 56. Wickersham IR, *et al.* (2015) Lentiviral vectors for retrograde delivery of recombinases
1027 and transactivators. *Cold Spring Harb Protoc* 2015(4):368-374.
- 1028 57. Sullivan HA & Wickersham IR (2015) Concentration and purification of rabies viral and
1029 lentiviral vectors. *Cold Spring Harb Protoc* 2015(4):386-391.
- 1030 58. Madisen L, *et al.* (2010) A robust and high-throughput Cre reporting and characterization
1031 system for the whole mouse brain. *Nature neuroscience* 13(1):133-140.
1032













Random 8-nucleotide index
Cre gene, P2A, mCherry gene, PEST, and transcription stop/polyA signal, transcription start signal, L gene, mutation

No mutations in transgene insert of SiR-CRE (19/21 clones)

ACTTTCTA, AGCCAGT, TTATCAGG, AGGGCGTT, AGTGGGCA, GGGCCTTT, TCCCGCAA, GGTCGGGG, GGCCTATA, TGTCTCTC, CCTGTCCG, TAGCACAC, GATGTGG, TAAGCCT, CTCACAT, TTAGTCC, AACCCGAC, AGCGGCC, AGCGGGG
CAACTCCAACCCCTGGGAGCAATATAACAAAAACATGTTATGGTGCCATTAAACCGCTGCATTTTCATCAAAGTCAAGTTGATTACCTTTACATTTTGATCCTCTTGGATGTGAAAAAACTATTAAACATCCCTCAAAGGACCTGCAGGTACGCGGCCGGTACCGCCACCATGGTGCCCAAGAAGAAGAGGAAAGTCTCCAACCTGCTGACTGTGCACCAAAACCTGCCTGCCCTCCCTGTGGATGCCACCTCTGATGAAGTCAGGAAGAACCTGATGGACATGTTTCAGGGACAGGCCAGCCTTCTGAACACACCTGGAAGATGCTCCTGTCTGTGTGCAGATCCTGGGCTGCCTGGTGAAGCTGAACAACAGAAATGGTTCCCTGCTGAACCTGAGGATGTGAGGGACTACCTCCTGTACCTGCAAGCAGAGGCCTGGCTGTGAAGACCATCCAACAGCACCTGGGCCAGCTCAACATGCTGCACAGGAGATCTGGCCTGCCTCGCCCTTCTGACTCCAATGCTGTGCCCTGGTGATGAGGAGAATCAGAAAGGAGAATGTGGATGCTGGGGAGAGAGCCAAAGAGCCCTTCCCTGGCATTGCTTACCAACACCTGCTGCGCATTGCCGAAATGCCAGAATCAGAGTGAAGGACATCTCCGCACCGATGGTGGGAGAATGCTGATCCACATTGGCAGGACCAAGACCCTGGTGTCCACAGCTGGTGTGGAGAAGGCCCTGTCCCTGGGGTTACCAAGCTGGTGGAGAGATGGATCTCTGTGTCTGGTGTGGCTGATGACCCCAACAACACTGTTCTGCCGGGTGAGAAAGAAATGGTGTGGCTGCCCTTCTGCCACCTCCCACTGTCCACCCGGCCCTGGAAGGGATCTTTGAGGCCACCCACCGCCTGATCTATGGTGCCAAGGATGACTCTGGCAGAGATACCTGGCCTGGTCTGGCCACTCTGCCAGAGTGGGTGCTGCCAGGGACATGGCCAGGGCTGGTGTGCCATCCCTGAAATCATGCAGGCTGGTGGCTGGACCAATGTGAACATTGTGATGAACATCAGAAACCTGGACTCTGAGACTGGGGCATGGTGAAGCTGCTCGAGGATGGGGACGGCAGTGGAGGATCCGGAGCCACGAATCTCTCTCTGTTAAAGCAAGCAGGAGACGTGGAAGAAAACCCCGGTCCTACCGGTGTGAGCAAGGGCGAGGAGGATAACATGGCCATCATCAAGGAGTTCATGCGCTTCAAGGTGCACATGGAGGGCTCCGTGAACGGCCACGAGTTCGAGATCGAGGGCGAGGGCGAGGGCCGCCCTACGAGGCCACCCAGACCAGCCAGCTGAAGGTGACCAAGGGTGGCCCTGCCCTTCCCTGCTGACATCTGCCCCCTCAGTTCATGTACGGCTCCAAGGCCTACGTGAAGCACC CGCCGACATCCCCGACTACTTGAAGCTGTCCCTCCCCGAGGGCTTCAAGTGGGAGCGCGTGTGAACCTCGAGCGGGCGGTGGTGAACCTGACCCAGGACTCCTCCCTGCAGGACGGCGAGTTCATCTACAAGGTGAAGCTGCGCGGCACCAACTTCCCTCCGACGGCCCCGTAATGCAGAAGAAGACCATGGGCTGGGAGGCCTCCTCCGACGGATGTACCCTGAGGACGGCGCCCTGAAGGGCGAGATCAAGCAGAGGCTGAAGCTGAAGGACGGCGGCCACTACGACGCTGAGGTCAAGACCACCTACAAGGCCAAGAAGCCCGTGCAGCTGCCGGCGCCTACAACGTCAACATCAAGTTGGACATCACCTCCACAACGAGGACTACACCATCGTGAACAGTACGAACCGCGCCGAGGGCCGCCACTCCACCGGGCGCATGGACGAGCTGTACAAGGATATCTCAGCCATGGCTTCCCGCCGAGGTTGGAGGAGCAAGATGATGGCACGCTGCCCATGCTCTGTGCCCAGGAGAGCGGGATGGACCGTCAACCTGCAGCCTGTGCTTCTGCTAGGATCAATGTGTGACTCGAGGGCGCGCTACCCGCGGTAGCTTTTCAAGTCAAGAAAAAACTTAGATCA GAAGAACAACCTGGCAACACTTCAACCTGAGACTTACTTCAAGATGCTCGATCCTGGAGAGGTCTATGATGACCCTATTGACCCAATCGAGTTAGAGGCTGAACCCAGAGGAACCCCATTTGCCCAAC

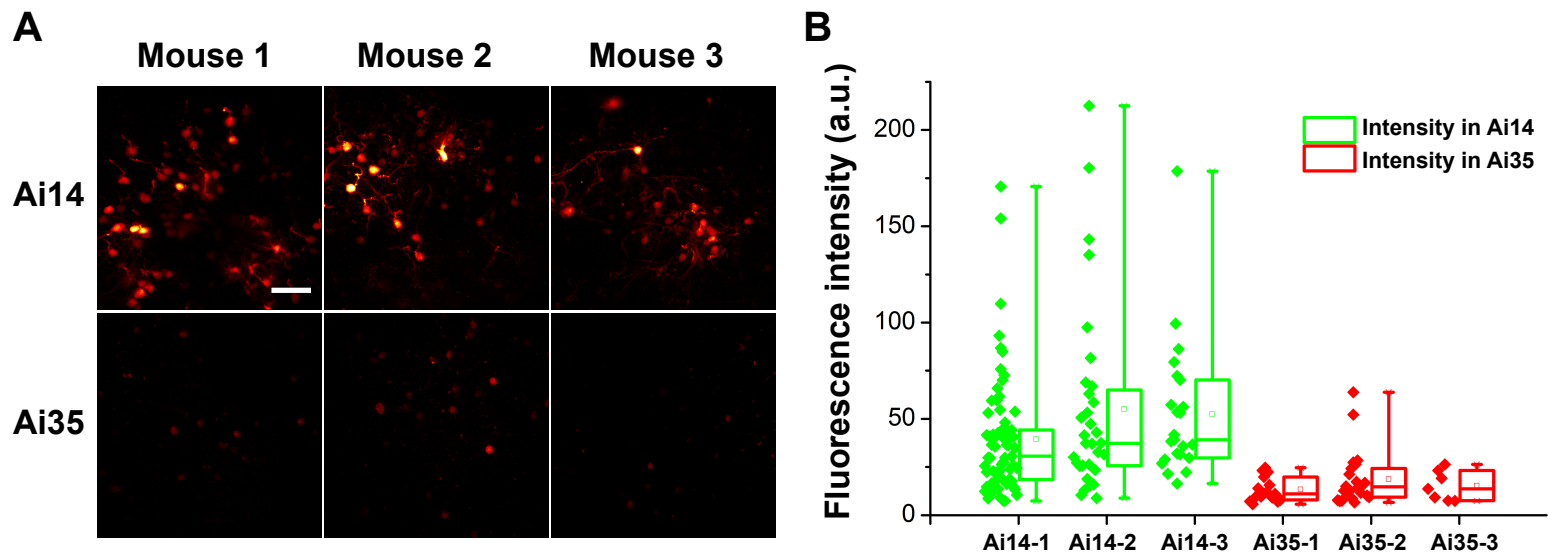
Ala88Val mutation in iCre gene of SiR-CRE (1/21 clones)

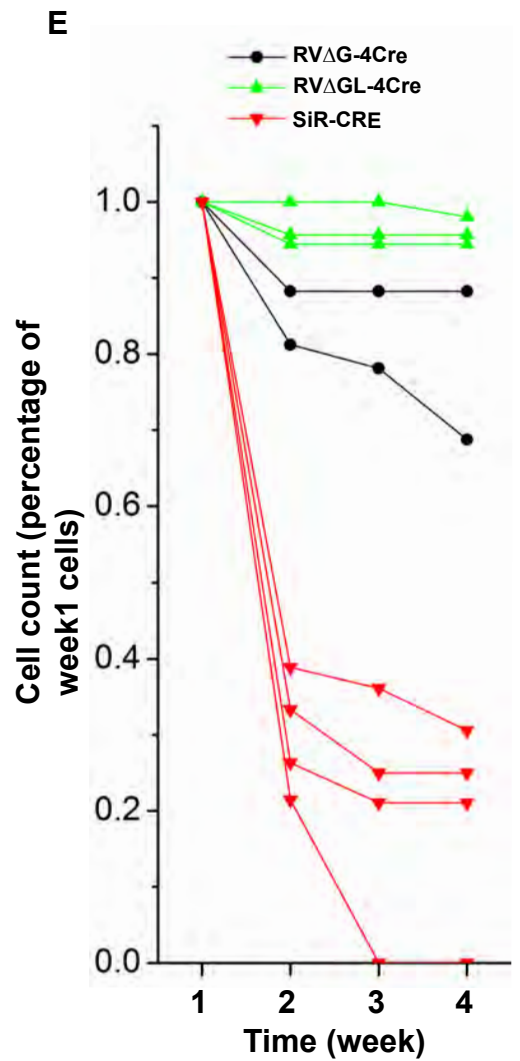
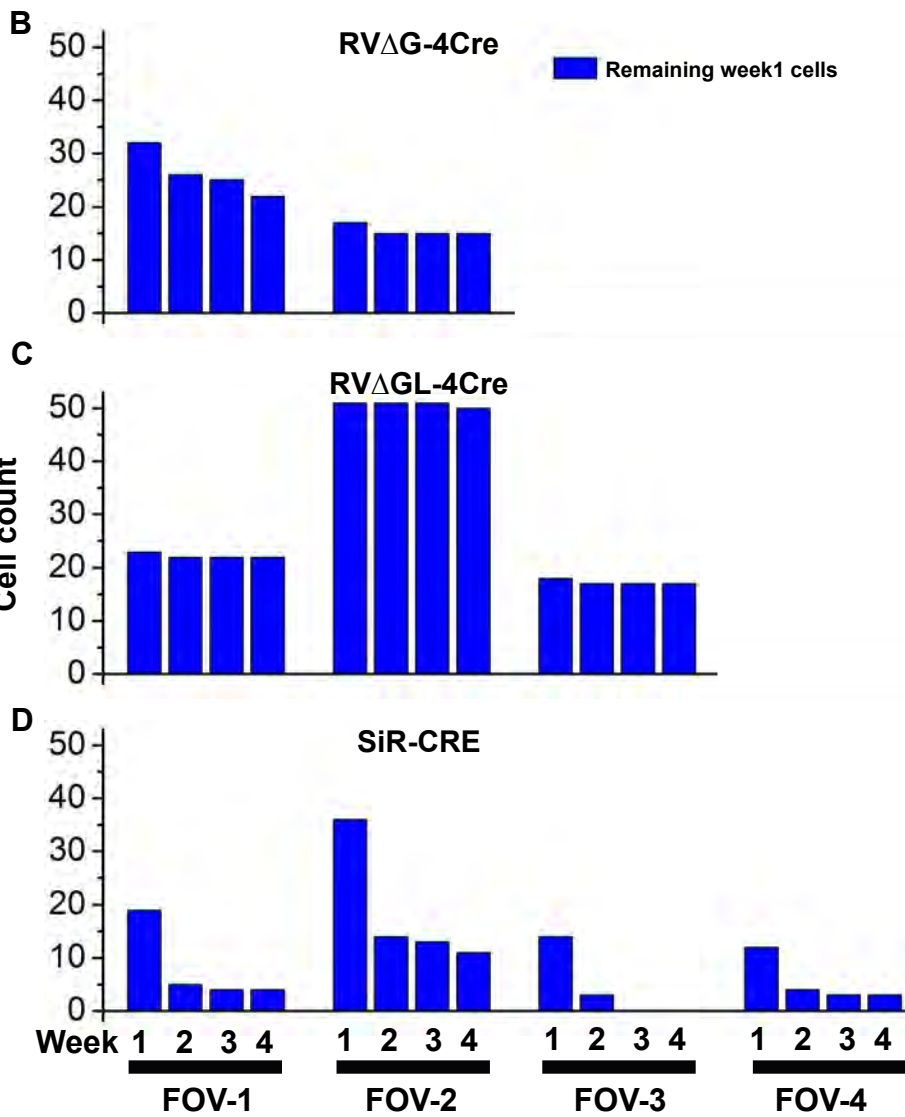
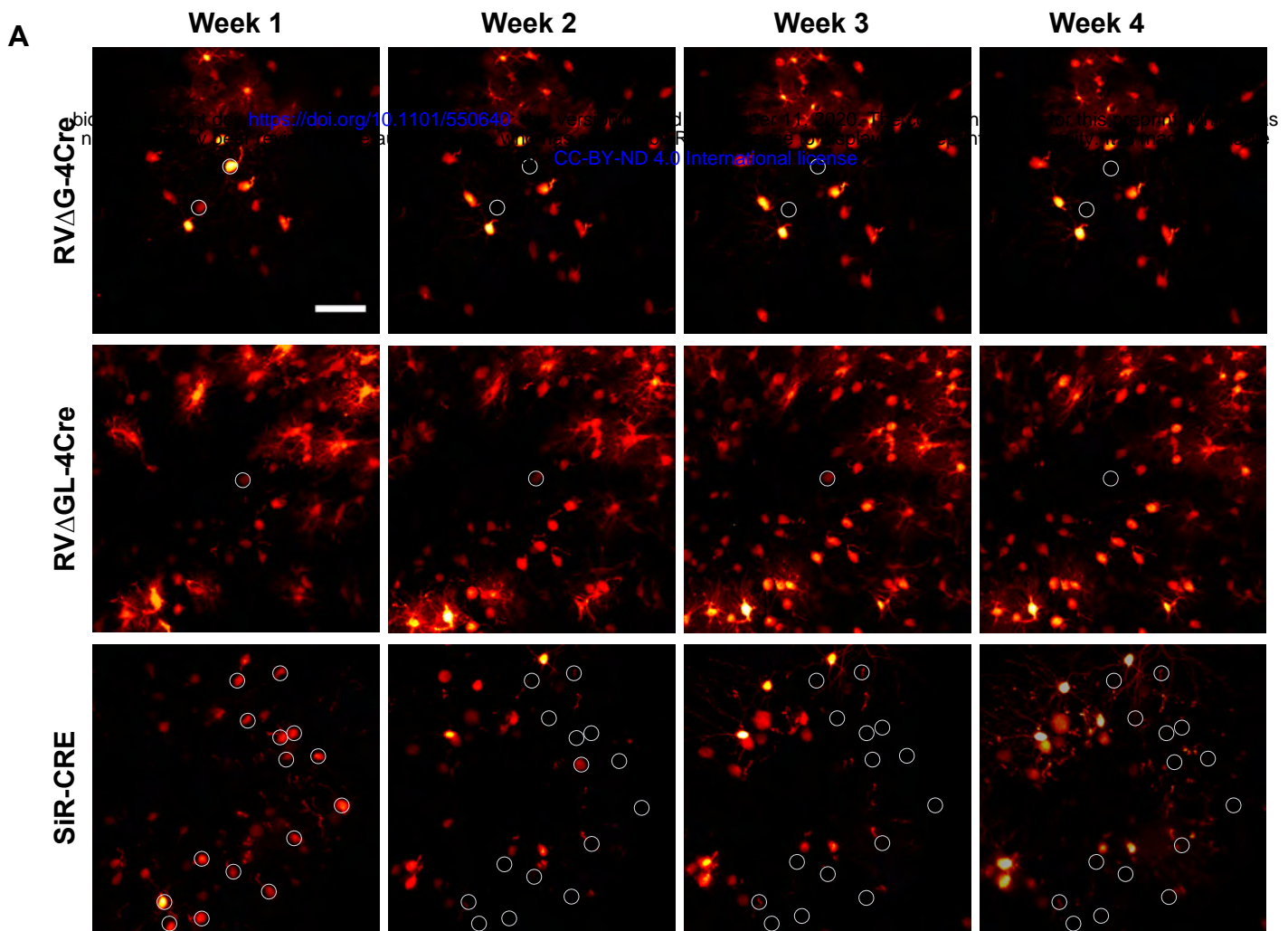
AGCTGGTT
CAACTCCAACCCCTGGGAGCAATATAACAAAAACATGTTATGGTGCCATTAAACCGCTGCATTTTCATCAAAGTCAAGTTGATTACCTTTACATTTTGATCCTCTTGGATGTGAAAAAACTATTAAACATCCCTCAAAGGACCTGCAGGTACGCGGCCGGTACCGCCACCATGGTGCCCAAGAAGAAGAGGAAAGTCTCCAACCTGCTGACTGTGCACCAAAACCTGCCTGCCCTCCCTGTGGATGCCACCTCTGATGAAGTCAGGAAGAACCTGATGGACATGTTTCAGGGACAGGCCAGCCTTCTGAACACACCTGGAAGATGCTCCTGTCTGTGTGCAGATCCTGGGCTGCCTGGTGAAGCTGAACAACAGAAATGGTTCCCTGCTGAACCTGAGGATGTGAGGGACTACCTCCTGTACCTGCAAGTCAGAGCCCTGGCTACAGGAATGGTTCCCTGCTGAACCTGAGGATGTGAGGGACTACCTCCTGTACCTGCAAGTCAGAGCCCTGGCTGTGAAGACCATCCAACAGCACCTGGGCCAGCTCAACATGCTGCACAGGAGATCTGGCCTGCCCTCGCCCTTCTGACTCCAATGCTGTGCCCTGGTGATGAGGAGAATCAGAAAGGAGAATGTGGATGCTGGGGAGAGAGCCAAGCAGCCCTGGCCTTGAACGCACTGACTTTGACCAAGTCAGATCCTGATGGAGAATCTGACAGATGCCAGGACATCAGGAACCTTCCCTGGCATTGCTTACCAACACCTGCTGCGCATTGCCGAAATGCCAGAATCAGAGTGAAGGACATCTCCCGACCGATGGTGGGAGAATGCTGATCCACATTGGCAGGACCAAGACCCTGGTGTCCACAGCTGGTGTGGAGAAGGCCCTGTCCCTGGGGTTACCAAGCTGGTGGAGAGATGGATCTCTGTGTCTGGTGTGGCTGATGACCCCAACAACACTGTTCTGCCGGGTGAGAAAGAAATGGTGTGGCTGCCCTTCTGCCACCTCCCAAGTGTCCACCCGGCCCTGGAAGGGATCTTTGAGGCCACCCACCGCCTGATCTATGGTGCCAAGGATGACTCTGGCAGAGATACCTGGCCTGGTCTGGCCACTTGCAGAGTGGTGTGCTGCCAGGGACATGGCCAGGCTGGTGTGCCATCCCTGAAATCATGCAGGCTGGTGGCTGGACCAATGTGAACATTGTGATGAACATCAGAAACCTGGA

```
CTCTGAGACTGGGGCCATGGTGAGGCTGCTCGAGGATGGGGACGGCAGTGGAGGATCCGGAGCCACGAACCTT
CTCTCTGTAAAGCAAGCAGGAGACGTGGAAGAAAACCCCGGTCTTACCGGTGTGAGCAAGGGCGAGGAGGAT
AACATGGCCATCATCAAGGAGTTCATGCGCTTCAAGGTGCACATGGAGGGCTCCGTGAACGGCCACGAGTTCGA
GATCGAGGGCGAGGGCGAGGGCCGCCCTACGAGGGCACCCAGACCGCCAAGCTGAAGGTGACCAAGGGTG
GCCCCCTGCCCTTCGCCCTGGGACATCCTGTCCCTCAGTTTCATGTACGGCTCCAAGGCCTACGTGAAGCACCC
CGCCGACATCCCGACTACTTGAAGCTGTCTTCCCGAGGGCTTCAAGTGGGAGCGCGTGATGAACTTCGAG
GACGGCGGCGTGGTGACCGTGACCCAGGACTCCTCCCTGCAGGACGGCGAGTTCATCTACAAGGTGAAGCTG
GCGGGCACCAACTTCCCTCCGACGGCCCCGTAATGCAGAAGAAGACCATGGGCTGGGAGGCCTCCTCCGAG
CGGATGTACCCGAGGACGGCGCCCTGAAGGGCGAGATCAAGCAGAGGCTGAAGCTGAAGGACGGCGGCCAC
TACGACGCTGAGGTCAAGACCACCTACAAGGCCAAGAAGCCCGTGCAGCTGCCGCGCCTACAACGTCAACA
TCAAGTTGGACATCACCTCCACAACGAGGACTACACCATCGTGAACAGTACGAACGCGCCGAGGGCCGCCA
CTCCACCGCGGCATGGACGAGCTGTACAAGGGATATCTCAGCCATGGCTTCCCGCCGGAGGTGGAGGAGCAG
GATGATGGCACGCTGCCCATGCTTGTGCCAGGAGAGCGGGATGGACCGTACCCTGCAGCCTGTGCTTCTG
CTAGGATCAATGTGTGACTCGAGGGCGCGCTACCCGCGGTAGCTTTTCAGTCTGAGAAAAAACATTAGATCAGA
AGAACAACTGGCAACACTTCTCAACCTGAGACTTACTTCAAGATGCTCGATCCTGGAGAGGTCTATGATGACCCT
ATTGACCCAATCGAGTTAGAGGCTGAACCCAGAGGAACCCCATTTGCCCAAC
```

Arg189Ile mutation in iCre gene of SiR-CRE

```
AGCGGGGT
CAACTCCAACCTTGGGAGCAATATAACAAAAACATGTTATGGTGCCATTAACCCGCTGCATTTTCATCAAAGTCA
AGTTGATTACCTTTACATTTTATCCTCTTGGATGTGAAAAAAACTATTAACATCCCTCAAAGGACCTGCAGGTACG
CGGCCGCGGTACCGCCACCATGGTGCCCAAGAAGAAGAGGAAAGTCTCCAACCTGCTGACTGTGCACAAAAAC
CTGCCTGCCCTCCCTGTGGATGCCACCTCTGATGAAGTCAGGAAGAACCTGATGGACATGTTTCAGGGACAGGCA
GGCCTTCTCTGAACACACCTGGAAGATGCTCCTGTCTGTGTGCAGATCCTGGGCTGCCTGGTGCAAGCTGAACA
ACAGGAAATGGTTCCCTGCTGAACCTGAGGATGTGAGGGACTACCTCCTGTACCTGCAAGCCAGAGGGCTGGC
TGTGAAGACCATCCAACAGCACCTGGGCCAGCTCAACATGCTGCACAGGAGATCTGGCCTGCCCTGCCCTTCT
GACTCCAATGCTGTGTCCCTGGTGATGAGGAGAATCAGAAAGGAGAATGTGGATGCTGGGGAGAGAGCCAAGC
AGGCCCTGGCCTTTGAACGCACTGACTTTGACCAAGTCAGATCCCTGATGGAGAACTCTGACAGATGCCAGGAC
ATCAGGAACCTGGCCTTCTGGGCATTGCCTACAACACCCTGCTGCGCATTGCCGAAATTGCCAGAATCAAGTG
AAGGACATCTCCCGCACCGATGGTGGGAGAATGCTGATCCACATTGGCAGGACCAAGACCCTGGTGTCCACAG
CTGGTGTGGAGAAGGCCCTGTCCCTGGGGGTTACCAAGCTGGTGGAGAGATGGATCTCTGTGTCTGGTGTGGC
TGATGACCCCAACAACCTACCTGTTCTGCCGGGTGAGAAAGAAATGGTGTGGCTGCCCTTCTGCCACCTCCCAAC
TGTCACCCGGGCCCTGGAAGGGATCTTTGAGGCCACCCACCGCTGATCTATGGTGCCAAGGATGACTCTGG
GCAGAGATACCTGGCCTGGTCTGGCCACTCTGCCAGAGTGGGTGCTGCCAGGGACATGGCCAGGGCTGGTGT
GTCCATCCCTGAAATCATGCAGGCTGGTGGCTGGACCAATGTGAACATTGTGATGAACTACATCAGAAACCTGGA
CTCTGAGACTGGGGCCATGGTGAGGCTGCTCGAGGATGGGGACGGCAGTGGAGGATCCGGAGCCACGAACCTT
CTCTCTGTAAAGCAAGCAGGAGACGTGGAAGAAAACCCCGGTCTTACCGGTGTGAGCAAGGGCGAGGAGGAT
AACATGGCCATCATCAAGGAGTTCATGCGCTTCAAGGTGCACATGGAGGGCTCCGTGAACGGCCACGAGTTCGA
GATCGAGGGCGAGGGCGAGGGCCGCCCTACGAGGGCACCCAGACCGCCAAGCTGAAGGTGACCAAGGGTG
GCCCCCTGCCCTTCGCCCTGGGACATCCTGTCCCTCAGTTTCATGTACGGCTCCAAGGCCTACGTGAAGCACCC
CGCCGACATCCCGACTACTTGAAGCTGTCTTCCCGAGGGCTTCAAGTGGGAGCGCGTGATGAACTTCGAG
GACGGCGGCGTGGTGACCGTGACCCAGGACTCCTCCCTGCAGGACGGCGAGTTCATCTACAAGGTGAAGCTG
CGGGCACCAACTTCCCTCCGACGGCCCCGTAATGCAGAAGAAGACCATGGGCTGGGAGGCCTCCTCCGAG
CGGATGTACCCGAGGACGGCGCCCTGAAGGGCGAGATCAAGCAGAGGCTGAAGCTGAAGGACGGCGGCCAC
TACGACGCTGAGGTCAAGACCACCTACAAGGCCAAGAAGCCCGTGCAGCTGCCGCGCCTACAACGTCAACA
TCAAGTTGGACATCACCTCCACAACGAGGACTACACCATCGTGAACAGTACGAACGCGCCGAGGGCCGCCA
CTCCACCGCGGCATGGACGAGCTGTACAAGGGATATCTCAGCCATGGCTTCCCGCCGGAGGTGGAGGAGCAG
GATGATGGCACGCTGCCCATGCTTGTGCCAGGAGAGCGGGATGGACCGTACCCTGCAGCCTGTGCTTCTG
CTAGGATCAATGTGTGACTCGAGGGCGCGCTACCCGCGGTAGCTTTTCAGTCTGAGAAAAAACATTAGATCAGA
AGAACAACTGGCAACACTTCTCAACCTGAGACTTACTTCAAGATGCTCGATCCTGGAGAGGTCTATGATGACCCT
ATTGACCCAATCGAGTTAGAGGCTGAACCCAGAGGAACCCCATTTGCCCAAC
```





Random 8-nucleotide index

N gene, tobacco etch virus protease cleavage site, PEST, transcription stop/polyA signal, mutation

Gly453* in N-TEV-PEST of SiR-CRE (50/51 clones)

TCTCGGAA, TTATGGGC, CCTGCCGA, CGTCGTTG, ACTCTAGT, GATCCGGT, ATTATGTA, TATTATCC, ATGCTAGA, GTTGTTTC, GAGTCGAC, GTCGACCT, CAAGAGTA, CGAAGCCA, GCGTGATA, CGTCCAGA, CTTGGTCC, GGGGTTTT, GTCCATAC, GTTTAATA, CAAAATCC, GTGGAGGC, CGGAAGGT, AGGACGGG, CCTCGGGA, GCATTTGC, TGGTTCGG, ATTTAGTC, ATGGGTAA, CTACGGGG, CCTGGTAC, GCATTTCA, AGTGTAGG, CGCATAGA, GTCACAAT, GTATGCTT, TCGGGTTT, ATGTTGTC, CAGCCGTA, GAGTGGCC, GGCCATT, GGATTTCC, GTACAAGC, GAAGATAT, AACAGAT, AAGGCCTT, CGTTCGTC, AAAGACTA, ACTGAAAG, TGGGGATA

ATCATCAAGCCCCTCCAAACTCATTGCGCCGAGTTTCTAAACAAGACATATTCGAGTGACTCAAGTTCCGAGAGA
ACCTCTACTTCCAATCGGGATCCGGTAGCCATGGCTTCCC GCCGGAGGTGGAGGAGCAGGATGATGGCACGCT
GCCCATGTCTTGTGCCAGGAGAGCGGGATGGACCGTACCCTGCAGCCTGTGCTTCTGCTAGGATCAATGTGT
AAGAAGTTGAATAACAAAATGCCGGAATCTACGGATTGTGTATATCCATCATGAAAAAAA

Asp449Glufs*16 in N-TEV-PEST of SiR-CRE (1/51 clones)

AGGCTAAC

ATCATCAAGCCCCTCCAAACTCATTGCGCCGAGTTTCTAAACAAGACATATTCGAGTGAACTCAAGTTCCGAGAGA
AACCTCTACTTCCAATCGGGATCCGGTAGCCATGGCTTCCC GCCGGAGGTGGAGGAGCAGGATGATGGCACGCT
TGCCCATGTCTTGTGCCAGGAGAGCGGGATGGACCGTACCCTGCAGCCTGTGCTTCTGCTAGGATCAATGTGT
TAAAGAAGTTGAATAACAAAATGCCGGAATCTACGGATTGTGTATATCCATCATGAAAAAAA

No mutations in sequenced region of N-TEV-PEST of SiR-FLPo (4/50 clones)

TCATTAT, AAGTCGAA, TGAATACA, TATACAGC

ATCATCAAGCCCCTCCAAACTCATTGCGCCGAGTTTCTAAACAAGACATATTCGAGTGACTCAAGTTCCGAGAGA
ACCTCTACTTCCAATCGGGATCCGGTAGCCATGGCTTCCC GCCGGAGGTGGAGGAGCAGGATGATGGCACGCT
GCCCATGTCTTGTGCCAGGAGAGCGGGATGGACCGTACCCTGCAGCCTGTGCTTCTGCTAGGATCAATGTGT
AAGAAGTTGAATAACAAAATGCCGGAATCTACGGATTGTGTATATCCATCATGAAAAAAA

Gly453* in N-TEV-PEST of SiR-FLPo (18/50 clones)

GAGGCCGC, CTTATCAC, TCAGTTTT, CTTAGCA, TTACTTTT, AAAATAAG, CCATTTCT, GTCACATT, GCATACGG, AGTATTAA, CCGGGTTG, GGTAATAA, CAGGGAGA, CATTITTC, TGACAAAT, TCGTATAT, TAGGGATT, GATCCCCG

ATCATCAAGCCCCTCCAAACTCATTGCGCCGAGTTTCTAAACAAGACATATTCGAGTGACTCAAGTTCCGAGAGA
ACCTCTACTTCCAATCGGGATCCGGTAGCCATGGCTTCCC GCCGGAGGTGGAGGAGCAGGATGATGGCACGCT
GCCCATGTCTTGTGCCAGGAGAGCGGGATGGACCGTACCCTGCAGCCTGTGCTTCTGCTAGGATCAATGTGT
AAGAAGTTGAATAACAAAATGCCGGAATCTACGGATTGTGTATATCCATCATGAAAAAAA

Ser450* in N-TEV-PEST of SiR-FLPo (28/50 clones)

TACTAAAT, TTCAACTA, TAATAGGC, CGCGGGTC, AGGGTGCC, TTGCTGAC, CGGCCCTT, TACAGCGA, GAGTAGGA, GTAAACGC, CTATGGGT, TTGATTGA, AGGATTCT, GAGGTTTG, TACTTAGC, CCTGTAGT, GGGGTGGA, TTAAGTTG, CTCAATGA, CAGATCTG, GTCTGGTA, GCGTTGGG, TAAACGAG, TACTTGAG, CGGGGTGT, CGATCCCG, TGGGTGTC, GCCACGAT

ATCATCAAGCCCCTCCAAACTCATTGCGCCGAGTTTCTAAACAAGACATATTCGAGTGACTCAAGTTCCGAGAGA
ACCTCTACTTCCAATCGGGATCCGGTAGCCATGGCTTCCC GCCGGAGGTGGAGGAGCAGGATGATGGCACGCT
GCCCATGTCTTGTGCCAGGAGAGCGGGATGGACCGTACCCTGCAGCCTGTGCTTCTGCTAGGATCAATGTGT
AAGAAGTTGAATAACAAAATGCCGGAATCTACGGATTGTGTATATCCATCATGAAAAAAA

No mutations in sequenced region of RVΔG-4mCherry (51/51 clones)

CGCCCCCG, GCCAATCT, GGCGGAAT, TGTGGAAC, GGAGGGAT, CGTAGTGT, AGAATCTC, TGTCTGGC, GCCTTTTA, TGGAACTC, TTGTAATG, AGGCCTGT, CGGATATA, AATCCAAA, AAGGAAAA, GAATCAT, GCCGCTTC, CTTTGCCG, CGCAACCT, TCGGGCAT, GGGCGACT, AACTGGAT, TCGTCCG, TCAAAGCG, CGAGGCC, ATGTAGGA, AGATACGT, TGGCTTCG, ATTTCTA, TCGTCCG, TCGGAGCG, CTGTTATA, TACCGTTC, CGAATGTC, CCCTTTT, TGAGTGGG, TGTAATA, AAGGAGTC, ATTACCCT, TCCCTGAC, TGGTAAA, ACTATCTC, CCGGAAGC, CTTGGAGG, GCAACAAT, ATTACCGT, AATAGCAG, ACCATAGT, GGGTTGGT, CATTATT, GGGTACAC

ATCATCAAGCCCCTCCAAACTCATTGCGCCGAGTTTCTAAACAAGACATATTCGAGTGACTCATAAAGAAGTTGAATA
ACAAAATGCCGGAATCTACGGATTGTGTATATCCATCATGAAAAAAA

SINGLE-MOLECULE, REAL-TIME SEQUENCING RESULTS

Frameshifts and insertions

Position numbers in this file refer to the reference sequences included as Supplementary Files S4-S5. A "frameshift" is included in Tables 1a-2b if the number of deleted bases in positions 1439-1492 (the vicinity of the junction of the end of the N gene and the intended 3' addition) is not an integer multiple of 3, with insertions ignored. "Any error" includes either the apparent frameshifts, or the new TAA/TAG/TGA stop codons, or both, with insertions ignored. The number of "frameshifts" increases considerably if insertion mutations are included in the calculation, indicating that there is a much higher insertion rate as compared to that of deletion; however, previous studies have found that spurious insertions are high with SMRT (see main text), so we ignore insertions in this paper apart from summarizing the data below.

SiR-CRE				
Position	Mutation	CCS3	CCS5	CCS8
# Sequences		22205	866	239
243	GAT (reference)	20273	784	209
	GCT	3	0	0
	GGT	5	0	0
	GTT	1856	79	29
	DEL	68	3	1
1111	GAA (reference)	19807	760	197
	GAC	1	0	0
	GAG	2396	105	42
	GAT	0	0	0
	DEL	1	1	0
1457	AGA	6	0	0
	CGA	1	0	0
	GGA (reference)	140	5	1
	TGA	22032	858	237
	DEL	26	3	1
[1439, 1492]	Frame shift (#DELs not an integer multiple of 3, Insertion ignored)	507	13	3
[1439, 1492]	Any error (insertion ignored)	22104	864	239
% mutation in [1439, 1492]		100%	100%	100%

Table 1a. All mutations in the SiR-CRE sample at positions mutated at >2% frequency at all stringencies (CCS3, CCS5, CCS8), as well as frameshift mutations found in the C-terminal region of N.

SiR-CRE				
Position	Mutation	CCS3	CCS5	CC8
[1439, 1492]	Number of frame shifts due to DEL (number of DELs not an integer multiple of 3, insertion ignored)	507	13	3
[1439, 1492]	Number of frame shifts due to either DEL or INS or both (Sequence length not an integer multiple of 3)	2504	89	14
[1439, 1492]	Any error (insertion included)	22174	865	239

Table 1b. Frameshift mutations in the C-terminal region of N in the SiR-CRE sample at positions mutated at >2% frequency at all stringencies (CCS3, CCS5, CCS8).

SiR-FLPo				
Position	Mutation	CCS3	CCS5	CCS8
#Sequences		17086	695	210
1449	TAA	28	1	0
	TCA (reference)	8405	333	94
	TGA	8624	360	115
	TTA	3	0	0
	DEL	26	1	1
1457	AGA	3	0	0
	CGA	0	0	0
	GGA (reference)	11088	462	139
	TGA	5979	233	71
	DEL	16	0	0
[1439, 1492]	Frameshifts (#DELS not an integer multiple of 3, Insertion ignored)	448	11	3
[1439, 1492]	Any error (insertion ignored)	14444	589	180
% of mutation		85%	85%	86%

Table 2a. All mutations in the SiR-FLPo sample at positions mutated at >2% frequency at all stringencies (CCS3, CCS5, CCS8), as well as frameshift mutations found in the C-terminal region of N.

SiR-FLPo				
Position	Mutation	CCS3	CCS5	CCS8
[1439, 1492]	Number of frame shifts due to DEL (number of DELs not an integer multiple of 3, insertion ignored)	448	11	3
[1439, 1492]	Number of frame shifts due to either DEL or INS or both (Sequence length not an integer multiple of 3)	3562	121	24
[1439, 1492]	Any error (insertion included)	15818	642	196

Table 2b. Frameshift mutations in the C-terminal region of N in the SiR-FLPo sample at positions mutated at >2% frequency at all stringencies (CCS3, CCS5, CCS8).

RV Δ G-4Cre				
Position	Mutation	CCS3	CCS5	CC8
# Sequences		17978	757	254
1355	ACT	1706	84	28
	CCT	3	0	0
	GCT	1	1	1
	TCT (reference)	16139	667	224
	DEL	129	5	1
Total				

Table 3. All mutations in the SiR-FLPo sample at positions mutated at >2% frequency at all stringencies (CCS3, CCS5, CCS8).

Tables of all mutations above 2% frequency threshold

Table 4a to 4c list all single-nucleotide substitutions and deletions at positions mutated at >2% threshold frequency. The percentage of mutations is calculated based on the total number of single nucleotide and deletion mutations divided by the total number of reads aligned, when insertion mutations are ignored. Deletion mutations dominate in the medium-frequency range between 2% and 5%.

	Reference	Position	A	C	G	T	DEL	Un-mutated	Mutated (SNP/DEL)	% Mutation (SNP/DEL)
CCS3	G	1457	6	1	140	22032	26	140	22065	99.4
	A	1111	19807	1	2396	0	1	19807	2398	10.8
	A	243	20273	3	5	1856	68	20273	1932	8.7
	T	615	4	0	2	21229	970	21229	976	4.4
	G	1124	5	0	21356	7	837	21356	849	3.8
	A	81	21358	9	2	0	836	21358	847	3.8
	A	31	21381	0	0	0	824	21381	824	3.7
	T	713	1	2	4	21487	711	21487	718	3.2
	T	338	0	0	9	21498	698	21498	707	3.2
	A	1665	21544	1	4	0	656	21544	661	3.0
	A	53	21606	0	0	1	598	21606	599	2.7
	C	411	8	21683	0	1	513	21683	522	2.4
A	838	21718	1	0	1	485	21718	487	2.2	
CCS5	G	1457	0	0	5	858	3	5	861	99.4
	A	1111	760	0	105	0	1	760	106	12.2
	A	243	784	0	0	79	3	784	82	9.5
	A	31	828	0	0	0	38	828	38	4.4
	G	1124	0	0	831	0	35	831	35	4.0
	T	615	0	0	0	834	32	834	32	3.7
	A	81	837	1	1	0	27	837	29	3.3
	T	338	0	0	1	840	25	840	26	3.0
	T	713	0	0	1	841	24	841	25	2.9
	C	411	0	843	0	0	23	843	23	2.7
	A	53	846	0	0	0	20	846	20	2.3
CCS8	G	1457	0	0	1	237	1	1	238	99.6
	A	1111	197	0	42	0	0	197	42	17.6
	A	243	209	0	0	29	1	209	30	12.6
	A	31	228	0	0	0	11	228	11	4.6
	T	615	0	0	0	232	7	232	7	2.9
	G	1124	0	0	232	0	7	232	7	2.9
C	411	0	233	0	0	6	233	6	2.5	

Table 4a. SiR-CRE: substitutions and deletions at positions mutated at >2% frequency at all stringencies (CCS3, CCS5, CCS8).

	Reference	Position	A	C	G	T	DEL	Un-mutated	Mutated (SNP/DEL)	% Mutation (SNP/DEL)
CCS3	C	1449	28	8405	8624	3	26	8405	8681	50.8
	G	1457	3	0	11088	5979	16	11088	5998	35.1
	T	615	4	0	0	16322	760	16322	764	4.5
	A	81	16410	4	2	5	665	16410	676	4.0
	G	1124	0	0	16410	3	673	16410	676	4.0
	T	713	1	0	2	16500	583	16500	586	3.4
	A	1665	16536	1	1	0	548	16536	550	3.2
	A	31	16547	0	0	0	539	16547	539	3.2
	T	338	0	1	4	16582	499	16582	504	2.9
	A	53	16672	2	2	0	410	16672	414	2.4
	C	411	6	16683	1	0	396	16683	403	2.4
	A	838	16696	0	0	0	390	16696	390	2.3
G	208	301	0	16739	44	2	16739	347	2.0	
CCS5	C	1449	1	333	360	0	1	333	362	52.1
	G	1457	0	0	462	233	0	462	233	33.5
	A	81	665	0	0	0	30	665	30	4.3
	T	615	1	0	0	668	26	668	27	3.9
	A	1665	669	0	1	0	25	669	26	3.7
	T	713	0	0	0	671	24	671	24	3.5
	T	338	0	0	0	673	22	673	22	3.2
	C	411	0	676	0	0	19	676	19	2.7
	G	1124	0	0	676	0	19	676	19	2.7
	A	838	679	0	0	0	16	679	16	2.3
	G	346	0	0	680	0	15	680	15	2.2
	A	31	681	0	0	0	14	681	14	2.0
CCS8	C	1449	0	94	115	0	1	94	116	55.2
	G	1457	0	0	139	71	0	139	71	33.8
	T	713	0	0	0	203	7	203	7	3.3
	A	53	205	0	0	0	5	205	5	2.4
	A	81	205	0	0	0	5	205	5	2.4

Table 4b. SiR-FLPo: substitutions and deletions at positions mutated at >2% frequency at all stringencies (CCS3, CCS5, CCS8).

	Reference	Position	A	C	G	T	DEL	Un-mutated	Mutated (SNP/DEL)	% Mutation (SNP/DEL)
CCS3	T	1355	1706	3	1	16139	129	16139	1839	10.2
	A	31	16732	0	0	0	1246	16732	1246	6.9
	T	615	2	0	1	17266	709	17266	712	4.0
	A	81	17300	4	2	1	671	17300	678	3.8
	G	1124	0	0	17379	4	595	17379	599	3.3
	T	713	0	1	1	17469	507	17469	509	2.8
	T	338	1	0	2	17503	472	17503	475	2.6
	A	1506	17520	0	0	0	458	17520	458	2.5
CCS5	A	53	17579	1	2	1	395	17579	399	2.2
	T	1355	84	0	1	667	5	667	90	11.9
	A	31	703	0	0	0	54	703	54	7.1
	A	81	717	0	0	0	40	717	40	5.3
	T	615	0	0	0	729	28	729	28	3.7
	G	1124	0	0	738	0	19	738	19	2.5
	A	53	739	0	0	0	18	739	18	2.4
	T	713	0	0	0	740	17	740	17	2.2
CCS8	A	1506	740	0	0	0	17	740	17	2.2
	T	1355	28	0	1	224	1	224	30	11.8
	A	31	241	0	0	0	13	241	13	5.1
	T	615	0	0	0	248	6	248	6	2.4

Table 4c. RVΔG-4Cre: substitutions and deletions at positions mutated at >2% frequency at all stringencies (CCS3, CCS5, CCS8).

LOCUS Exported 2183 bp ds-DNA linear SYN
07-JAN-2019
DEFINITION synthetic linear DNA.
ACCESSION .
VERSION .
KEYWORDS .
SOURCE synthetic DNA construct
ORGANISM synthetic DNA construct
REFERENCE 1 (bases 1 to 2183)
AUTHORS Trial User
TITLE Direct Submission
JOURNAL Exported Jan 7, 2019 from SnapGene 4.1.9
<http://www.snapgene.com>

FEATURES Location/Qualifiers
source 1..2183
/organism="PCR product"
/mol_type="other DNA"
primer_bind 1..48
/label=Barcode5_cagc_N10_leader_fp
primer_bind 1..20
/label=Barcode5_cagc_fp
gap 21..30
/estimated_length=10
5'UTR 31..100
/label=RV leader
/note="SPBN leader"
CDS 101..1450
/codon_start=1
/locus_tag="N"
/label=N
/note="N"
/
translation="MDADKIVFKVNNQVVSLKPEIIVDQY EYKYP AIKDLKKPCITLGK
APDLNKAYKSVLSGMSAAKLNPDVCSYLAAMQFFEGT
CPEDWTSYGIVIARKGDKIT
PGSLVEIKRTDVEGNWAL TGGMELTRDPTV
PEHASLVGLLLSLYRLSKISGQNTGNYKT
NIADRIEQIFETAPFVKIVEHHTLMTTHKMCAN
WSTIPNFRFLAGTYDMFFSRIEHLYS
AIRVGT VVTAYEDCSGLVSFTGFIKQINLTARE
AILYFFHKNFEEEEIRRMFEPGQETAV
PHSYFIHFRSLGLSGKSPYSSNAVGHVFNLIHF
VGCYMGQVRSLNATVIAACAPHEMSV
LGGYLGEFFGKGT FERRFRDEKELQEYEAEL
TKTDVALADDGTVNSDDEDYFSGET
RSPEAVYTRIMMNGGRLKRSHIRRYVS
VSSNHQARPNSFAEFLNKTYSSDS"
CDS 1460..1480
/codon_start=1
/locus_tag="TEV site"

```

                                /label=TEV site
                                /note="TEV site"
                                /translation="ENLYFQS"
CDS                               1490..1609
                                /codon_start=1
                                /locus_tag="ECFP destabilized by fusion to
residues 422-461                 of mouse ornithine decarboxylase, giving an in
vivo(1)"                         /product="ECFP destabilized by fusion to residues
422-461                          of mouse ornithine decarboxylase, giving an in
vivo                              half-life of ~2 hours"
422-461                          /label=ECFP destabilized by fusion to residues
422-461...                      /label=ECFP destabilized by fusion to residues
422-461 of                       mouse ornithine decarboxylase, giving an in
vivo(1)                          /note="destabilization domain"
                                /note="mammalian codon-optimized"
                                /
translation="SHGFPPEVEEQDDGTLPMSCAQESGMDRHPAACASARINV"
CDS                               1703..2167
                                /codon_start=1
                                /locus_tag="P"
                                /label=P
                                /note="P"
                                /
translation="MSKIFVNPSAIRAGLADLEMAEETVDLINRNIEDNQAHLQGEPIE
VDNLPEDMGRHLHDDGKSPNHGEIAKVGEGKYREDFQMDEGEDPSFLFQSYLENVGVQI
VRQMRSGERFLKIWSQTVEEIISYVAVNFPNPPGKSSDKSTQTTGRELKK"
primer_bind      complement(2148..2183)
                                /label=Barcode3_P_rp
ORIGIN
    1 acacgcatga cacactcagc nnnnnnnnnn acgcttaaca accagatcaa
agaaaaaaca
    61 gacattgtca attgcaaagc aaaaatgtaa caccctaca atggatgccg
acaagattgt
   121 attcaaagtc aataatcagg tggctctctt gaagcctgag attatcgtgg
atcaatatga
   181 gtacaagtac cctgccatca aagatttgaa aaagccctgt ataaccctag
gaaaggctcc
   241 cgatttaa ataaagcataca agtcagtttt gtcaggcatg agcgccgcca
aacttaatcc
```

301 tgacgatgta tgttcctatt tggcagcggc aatgcagttt tttgagggga
catgtccgga
361 agactggacc agctatggaa ttgtgattgc acgaaaagga gataagatca
ccccaggttc
421 tctggtggag ataaaacgta ctgatgtaga agggaattgg gctctgacag
gaggcatgga
481 actgacaaga gaccccactg tccctgagca tgcgtcctta gtcggtcttc
tcttgagtct
541 gtataggttg agcaaaatat ccgggcaaaa cactggtaac tataagacaa
acattgcaga
601 caggatagag cagatTTTTG agacagcccc ttttgTtaaa atcgtggaac
accatactct
661 aatgacaact cacaaaatgt gtgctaattg gagtactata ccaaacttca
gatttttggc
721 cggaacctat gacatgtttt tctcccggat tgagcatcta tattcagcaa
tcagagtggg
781 cacagttgtc actgcttatg aagactgttc aggactggta tcatttactg
ggttcataaa
841 acaaatcaat ctaccgcta gagaggcaat actatatttc ttccacaaga
actttgagga
901 agagataaga agaatgtttg agccagggca ggagacagct gttcctcact
cttatttcat
961 ccacttccgt tcaactaggct tgagtgggaa atctccttat tcatcaaatg
ctgttggtca
1021 cgtgttcaat ctcaattcact ttgtaggatg ctatatgggt caagtccgat
ccctaaatgc
1081 aacggttatt gctgcatgtg ctctcatga aatgtctggt ctagggggct
atctgggaga
1141 ggaattcttc gggaaagggga catttgaaag aagattcttc agagatgaga
aagaacttca
1201 agaatacagag gcggctgaac tgacaaagac tgacgtagca ctggcagatg
atggaactgt
1261 caactctgac gacgaggact acttttcagg tgaaaccaga agtccggagg
ctgtttatac
1321 tcgaatcatg atgaatggag gtcgactaaa gagatctcac atacggagat
atgtctcagt
1381 cagttccaat catcaagccc gtccaaactc attcgccgag tttctaaaca
agacatattc
1441 gagtgactca ggttccggag agaacctcta cttccaatcg ggatccggta
gccatggctt
1501 cccgccggag gtggaggagc aggatgatgg cacgctgcc atgtcttgtg
cccaggagag
1561 cgggatggac cgtcaccctg cagcctgtgc ttctgctagg atcaatgtgt
aagaagttga
1621 ataacaaaat gccggaaatc tacggattgt gtatatccat catgaaaaaa
actaacaccc
1681 ctcctttcga accatcccaa acatgagcaa gatctttgtc aatcctagtg
ctattagagc
1741 cggctctggcc gatcttgaga tggctgaaga aactgttgat ctgatcaata
gaaatatcga

```
1801 agacaatcag gctcatctcc aaggggaacc catagaggtg gacaatctcc
ctgaggatat
1861 ggggcgactt cacctggatg atggaaaatc gcccaacat ggtgagatag
ccaaggtggg
1921 agaaggcaag tatcgagagg actttcagat ggatgaagga gaggatccta
gcttcctggt
1981 ccagtcatac ctggaaaatg ttggagtcca aatagtcaga caaatgaggt
caggagagag
2041 atttctcaag atatggtcac agaccgtaga agagattata tcctatgtcg
cggtcaactt
2101 tcccaaccct ccaggaaagt cttcagagga taaatcaacc cagactactg
gccgagagct
2161 caagaagtac tagagtagca ctc
//
```


LOCUS Exported 2183 bp ds-DNA linear SYN
07-JAN-2019
DEFINITION synthetic linear DNA.
ACCESSION .
VERSION .
KEYWORDS .
SOURCE synthetic DNA construct
ORGANISM synthetic DNA construct
REFERENCE 1 (bases 1 to 2183)
AUTHORS Trial User
TITLE Direct Submission
JOURNAL Exported Jan 7, 2019 from SnapGene 4.1.9
<http://www.snapgene.com>

FEATURES Location/Qualifiers
source 1..2183
/organism="synthetic DNA construct"
/mol_type="other DNA"
primer_bind 1..48
/label=Barcode9_cagc_N10_leader_fp
primer_bind 1..20
/label=Barcode9_cagc_fp
gap 21..30
/estimated_length=10
5'UTR 31..100
/label=RV leader
/note="SPBN leader"
misc_feature 89..97
/label=Transcription start signal (N)
CDS 101..1450
/codon_start=1
/locus_tag="N"
/label=N
/note="N"
/
translation="MDADKIVFKVNNQVVSLKPEIIVDQY EYKYP AIKDLKKPCITL GK
APDLNKAYKSVLSGMSAAKLNPDVCSYLAAMQFFEGT CPEDWTSY GIVIARKGDKIT
PGSLVEIKRTDVEGNWALTGGMELTRDPTVPEHASLVGLLLSLYRLSKISGQNTGNYKT
NIADRIEQIFETAPFVKIVEHHTLMTTHKMCANWSTIPNFRFLAGTYDMFFSRIEHLYS
AIRVGT VVTAYEDCSGLVSFTGFIKQINLTAREAILYFFHKNFEEEIRRMFEPGQETAV
PHSYFIHFRSLGLSGKSPYSSNAVGHVFNL IHFVGCYMGQVRSLNATVIAACAPHEMSV
LGGYLGEFFGKGT FERRFRDEKELQEYEA AELTKTDVALADDGTVNSDDEDYFSGET
RSPEAVYTRIMMNGGRLKRSHIRRYVSVSSNHQARPNSFAEFLNKTYSSDS"
CDS 1460..1480

```

/codon_start=1
/product="tobacco etch virus (TEV) protease
recognition and
cleavage site"
/label=TEV site
/translation="ENLYFQS"
CDS
1490..1609
/codon_start=1
/locus_tag="ECFP destabilized by fusion to
residues 422-461
of mouse ornithine decarboxylase, giving an in
vivo(1)"
/product="ECFP destabilized by fusion to residues
422-461
of mouse ornithine decarboxylase, giving an in
vivo
half-life of ~2 hours"
/label=PEST
/label=ECFP destabilized by fusion to residues
422-461 of
mouse ornithine decarboxylase, giving an in
vivo(1)
/note="destabilization domain"
/note="mammalian codon-optimized"
/
translation="SHGFPPEVEEQDDGTLPMSCAQESGMDRHPAACASARINV"
misc_feature 1661..1671
/label=Transcription stop/pA signal (N/P & P/M))
misc_feature 1674..1682
/label=Transcription start signal (P)
misc_feature 1703..2167
/locus_tag="P"
/label=P
/note="P"
primer_bind complement(2148..2183)
/label=Barcode4_P_rp
ORIGIN
1 ctgcgtgctc tacgaccagc nnnnnnnnnn acgcttaaca accagatcaa
agaaaaaaca
61 gacattgtca attgcaaagc aaaaatgtaa caccctaca atggatgccg
acaagattgt
121 attcaaagtc aataatcagg tggctctctt gaagcctgag attatcgtgg
atcaatatga
181 gtacaagtac cctgccatca aagatttgaa aaagccctgt ataaccctag
gaaaggctcc
241 cgatttaa ataaagcataca agtcagtttt gtcaggcatg agcgccgcca
aacttaaatcc
301 tgacgatgta tgttcctatt tggcagcggc aatgcagttt tttgagggga
catgtccgga
361 agactggacc agctatggaa ttgtgattgc acgaaaagga gataagatca
```

ccccagggttc
421 tctggtggag ataaaacgta ctgatgtaga agggaattgg gctctgacag
gaggcatgga
481 actgacaaga gaccccactg tccctgagca tgcgctccta gtcggtcttc
tcttgagtct
541 gtatagggtg agcaaaatat ccgggcaaaa cactggtaac tataagacaa
acattgcaga
601 caggatagag cagatTTTTG agacagcccc ttttgTtaaa atcgtggaac
accatactct
661 aatgacaact cacaaaatgt gtgctaattg gagtactata ccaaacttca
gatttttggc
721 cggaacctat gacatgtttt tctcccggat tgagcatcta tattcagcaa
tcagagtggg
781 cacagttgtc actgcttatg aagactgttc aggactggta tcatttactg
ggttcataaa
841 acaaatcaat ctcaccgcta gagaggcaat actatatttc ttccacaaga
actttgagga
901 agagataaga agaatgtttg agccagggca ggagacagct gttcctcact
cttatttcat
961 ccacttccgt tccactaggct tgagtgggaa atctccttat tcatcaaatg
ctgttggtca
1021 cgtgttcaat ctcattcact ttgtaggatg ctatatgggt caagtcagat
ccctaaatgc
1081 aacggttatt gctgcatgtg ctctcatga aatgtctgtt ctagggggct
atctgggaga
1141 ggaattcttc gggaaaggga catttgaaag aagattcttc agagatgaga
aagaacttca
1201 agaatacgag gcggtgaac tgacaaagac tgacgtagca ctggcagatg
atggaactgt
1261 caactctgac gacgaggact acttttcagg tgaaccaga agtccggagg
ctgtttatac
1321 tcgaatcatg atgaatggag gtcgactaaa gagatctcac atacggagat
atgtctcagt
1381 cagttccaat catcaagccc gtccaaactc attcgccgag tttctaaaca
agacatatc
1441 gagtgactca ggttccggag agaacctcta cttccaatcg ggatccggta
gccatggctt
1501 cccgccggag gtggaggagc aggatgatgg cacgctgcc atgtcttgtg
cccaggagag
1561 cgggatggac cgtcaccctg cagcctgtgc ttctgctagg atcaatgtgt
aagaagttga
1621 ataacaaaat gccggaaatc tacggattgt gtatatccat catgaaaaa
actaacacc
1681 ctcctttcga accatcccaa acatgagcaa gatctttgtc aatcctagtg
ctattagagc
1741 cggctctggcc gatcttgaga tggctgaaga aactgttgat ctgatcaata
gaaatatcga
1801 agacaatcag gctcatctcc aagggaacc catagagggtg gacaatctcc
ctgaggatat
1861 ggggcgactt cacctggatg atggaaaatc gcccaacat ggtgagatag

```
ccaaggtggg
  1921 agaaggcaag tatcgagagg actttcagat ggatgaagga gaggatccta
gcttcctggt
  1981 ccagtcatac ctggaaaatg ttggagtcca aatagtcaga caaatgaggt
caggagagag
  2041 atttctcaag atatggtcac agaccgtaga agagattata tcctatgtcg
cggtcaactt
  2101 tcccaaccct ccaggaaagt cttcagagga taaatcaacc cagactactg
gccgagagct
  2161 caagaagtgt gtatcagtac atg
//
```

LOCUS Exported 2024 bp ds-DNA linear SYN
07-JAN-2019
DEFINITION synthetic linear DNA.
ACCESSION .
VERSION .
KEYWORDS .
SOURCE synthetic DNA construct
ORGANISM synthetic DNA construct
REFERENCE 1 (bases 1 to 2024)
AUTHORS Trial User
TITLE Direct Submission
JOURNAL Exported Jan 7, 2019 from SnapGene 4.1.9
<http://www.snapgene.com>

FEATURES Location/Qualifiers
source 1..2024
/organism="synthetic DNA construct"
/mol_type="other DNA"
primer_bind 1..48
/label=Barcode1_cagc_N10_leader_fp
primer_bind 1..20
/label=Barcode1_cagc_fp
gap 21..30
/estimated_length=10
5'UTR 31..100
/label=RV leader
/note="SPBN leader"
misc_feature 89..97
/locus_tag="Transcriptional start (N)"
/label=Transcriptional start (N)
CDS 101..1450
/codon_start=1
/locus_tag="N"
/label=N
/note="N"
/
translation="MDADKIVFKVNNQVVSLKPEIIVDQYQYKYP AIKDLKKPCITL GK
APDLNKAYKSVLSGMSAAKLNPDVCSYLAAMQFFEGTCPEDWTSYGIVIARKGDKIT
PGSLVEIKRTDVEGNWALTGGMELTRDPTVPEHASLVGLLLSLYRLSKISGQNTGNYKT
NIADRIEQIFETAPFVKIVEHHTLMTTHKMCANWSTIPNFRFLAGTYDMFFSRIEHLYS
AIRVGTVVTAYEDCSGLVSFTGFIKQINLTAREAILYFFHKNFEEEIRRMFEPGQETAV
PHSYFIHFRSLGLSGKSPYSSNAVGHVFNLIHFVGCYMGQVRSLNATVIAACAPHEMSV
LGGYLGEFFGKGTERRFFRDEKELQEYEAELTKTDVALADDGTVNSDDEDYFSGET
RSPEAVYTRIMMNGGRLKRSHIRRYVSVSSNHQARPNSFAEFLNKTYSSDS"

misc_feature 1502..1512
/label=Transcription stop/pA signal (N/P & P/M))
misc_feature 1515..1523
/locus_tag="Transcriptional start (P)"
/label=Transcriptional start (P)
misc_feature 1544..2008
/locus_tag="P"
/label=P
/note="P"
primer_bind complement(1989..2024)
/label=Barcode2_P_rp

ORIGIN

1 tcagacgatg cgtcatcagc nnnnnnnnnn acgcttaaca accagatcaa
agaaaaaaca
61 gacattgtca attgcaaagc aaaaatgtaa caccctaca atggatgccg
acaagattgt
121 attcaaagtc aataatcagg tggctctctt gaagcctgag attatcgtgg
atcaatatga
181 gtacaagtac cctgccatca aagatttgaa aaagccctgt ataaccctag
gaaaggctcc
241 cgatttaaataaagcataca agtcagtttt gtcaggcatg agcgccgcca
aacttaatcc
301 tgacgatgta tgttcctatt tggcagcggc aatgcagttt tttgagggga
catgtccgga
361 agactggacc agctatggaa ttgtgattgc acgaaaagga gataagatca
ccccaggttc
421 tctggtggag ataaaacgta ctgatgtaga aggaattgg gctctgacag
gaggcatgga
481 actgacaaga gaccccactg tccctgagca tgcgtcctta gtcggtcttc
tcttgagtct
541 gtataggttg agcaaatat cggggcaaaa cactggtaac tataagacaa
acattgcaga
601 caggatagag cagatTTTTG agacagcccc ttttgTtaaa atcgtggaac
accatactct
661 aatgacaact cacaaaatgt gtgctaattg gagtactata ccaaacttca
gatttttggc
721 cggaacctat gacatgtttt tctcccggat tgagcatcta tattcagcaa
tcagagtggg
781 cacagttgtc actgcttatg aagactgttc aggactggta tcatttactg
ggttcataaa
841 acaaatcaat ctcaccgcta gagaggcaat actatatttc ttccacaaga
actttgagga
901 agagataaga agaatgtttg agccagggca ggagacagct gttcctcact
cttatttcat
961 ccacttccgt tcactaggct tgagtgggaa atctccttat tcatcaaatg
ctgttggtca
1021 cgtgttcaat ctcatcact ttgtaggatg ctatatgggt caagtcagat
ccctaaatgc
1081 aacggttatt gctgcatgtg ctctcatga aatgtctggt ctagggggct
atctgggaga

```
1141 ggaattcttc gggaaagga catttgaag aagattcttc agagatgaga
aagaacttca
1201 agaatacgag gcggctgaac tgacaaagac tgacgtagca ctggcagatg
atggaactgt
1261 caactctgac gacgaggact acttttcagg tgaaaccaga agtccggagg
ctgtttatac
1321 tcgaatcatg atgaatggag gtcgactaaa gagatctcac atacggagat
atgtctcagt
1381 cagttccaat catcaagccc gtccaaactc attcgccgag tttctaaaca
agacatatc
1441 gagtgactca taagaagttg aataacaaaa tgccggaaat ctacggattg
tgtatatcca
1501 tcatgaaaaa aactaacacc cctcctttcg aaccatcca aacatgagca
agatctttgt
1561 caatcctagt gctattagag ccggtctggc cgatcttgag atggctgaag
aaactgttga
1621 tctgatcaat agaaatatcg aagacaatca ggctcatctc caaggggaac
ccatagaggt
1681 ggacaatctc cctgaggata tggggcgact tcacctggat gatggaaaat
cgcccaacca
1741 tggtagagata gccaaggtgg gagaaggcaa gtatcgagag gactttcaga
tggatgaagg
1801 agaggatcct agcttcctgt tccagtcata cctggaaaat gttggagtcc
aaatagtcag
1861 acaaatgagg tcaggagaga gatttctcaa gatatgggtca cagaccgtag
aagagattat
1921 atcctatgtc gcggtcaact ttccaaccc tccaggaaag tcttcagagg
ataaatcaac
1981 ccagactact ggccgagagc tcaagaagct atacatgact ctgc
//
```

